A rapid and high-precision mountain vertex extraction method based on hotspot analysis clustering and improved eight-connected extraction algorithms for digital elevation models

Zheng, Zhenqi; Xiao, Xiongwu; Zhong, Zhi Chao; Zang, Yufu; Yang, Nan; Tu, Jianguang; Li, Deren

DOI
10.3390/rs13010081

Publication date
2021

Document Version
Final published version

Published in
Remote Sensing

remote sensing

MDPI

Article

A Rapid and High-Precision Mountain Vertex Extraction Method Based on Hotspot Analysis Clustering and Improved Eight-Connected Extraction Algorithms for Digital Elevation Models

Zhenqi Zheng [1,2,†], Xiongwu Xiao [3,4,*], Zhi-Chao Zhong [1,3,†], Yufu Zang [5,6,†], Nan Yang [7] and Jianguang Tu [1] and Deren Li [1,3,4]

1 School of Remote Sensing and Information Engineering, Wuhan University, Wuhan 430079, China; zhengzhenqi@whu.edu.cn (Z.Z.); 2015302580158@whu.edu.cn (Z.-C.Z.); Tu.Jianguang@whu.edu.cn (J.T.); drli@whu.edu.cn (D.L.)
2 Wuhan Headquarters of Xiaomi Co., LTD, Wuhan 430079, China
3 State Key Laboratory of Information Engineering in Surveying, Mapping and Remote Sensing, Wuhan University, Wuhan 430079, China
4 Collaborative Innovation Center for Geospatial Technology, Wuhan 430079, China
5 Remote Sensing & Geomatics Engineering, Nanjing University of Information Science & Technology, 219 Ningliu Road, Nanjing 210044, China; 3dmapzangyufu@nuist.edu.cn
6 Department of Geoscience and Remote Sensing, Delft University of Technology, Stevinweg 1, 2628 CN Delft, The Netherlands
7 School of Transportation Science and Engineering, Harbin Institute of Technology, Harbin 150090, China; nyang24@hit.edu.cn
* Correspondence: xwxiao@whu.edu.cn; Tel.: +86-186-0276-2010
† These authors contributed equally to this work.

Citation: Zheng, Z.; Xiao, X.; Zhong, Z.-C.; Zang, Y.; Yang, N.; Tu, J.; Li, D. A Rapid and High-Precision Mountain Vertex Extraction Method Based on Hotspot Analysis Clustering and Improved Eight-Connected Extraction Algorithms for Digital Elevation Models. *Remote Sens.* **2021**, *13*, 81. https://doi.org/10.3390/rs13010081

Received: 7 November 2020
Accepted: 24 December 2020
Published: 28 December 2020

Abstract: Digital Elevation Model (DEM)-based mountain vertex extraction is one of the most useful DEM applications, providing important information to properly characterize topographic features. Current vertex-extraction techniques have considerable limitations, such as yielding low-accuracy results and generating false mountain vertices. To overcome these limitations, a new approach is proposed that combines Hotspot Analysis Clustering and the Improved Eight-Connected Extraction algorithms that would quickly and accurately provide the location and elevation of mountain vertices. The use of the elevation-based Hotspot Analysis Clustering Algorithm allows the fast partitioning of the mountain vertex area, which significantly reduces data and considerably improves the efficiency of mountain vertex extraction. The algorithm also minimizes false mountain vertices, which can be problematic in valleys, ridges, and other rugged terrains. The Eight-Connected Extraction Algorithm also hastens the precise determination of vertex location and elevation, providing a better balance between accuracy and efficiency in vertex extraction. The proposed approach was used and tested on seven different datasets and was compared against traditional vertex extraction methods. The results of the quantitative evaluation show that the proposed approach yielded higher efficiency, considerably minimized the occurrence of invalid points, and generated higher vertex extraction accuracy compared to other traditional methods.

Keywords: mountain vertex extraction; Hotspot Analysis Clustering; Improved Eight-Connected Algorithm; Contour Line Method; Contour Line and Neighborhood Analysis Overlay Method; Digital Elevation Model (DEM)

1. Introduction

Digital Elevation Model (DEM) is a physical model depicting ground elevations using ordered numerical arrays and exists in several data formats (e.g., raster, vector, TIN, point cloud). DEM is usually defined in 2.5D, with 2D plane coordinates (x, y) and an elevation

attribute (h). DEM is a form of digital terrain model (DTM) that describes the spatial distribution of various geomorphic factors, such as slope, slope direction, and slope change rate. DEM is a zero-order single digital geomorphic model, which can be used to generate other geomorphic factors [1,2]. The generation methods can be roughly divided into two categories. First is using photogrammetric processing technology [3,4] to directly generate DEM by processing images from satellites [5], aircraft [6], UAV [7], and other platforms. The second is using contour lines and elevation point data, constructed through high-precision GNSS [8] and laser scanning [9,10], to establish the irregular triangular network and use bilinear or inverse distance interpolation algorithm to generate the DEM [11]. Compared with conventional maps, the DEM is characterized by high data accuracy, easy calculations, and diverse expression forms [12]. It can efficiently produce multiple terrain factors, such as the mountain vertex, slope, aspect, mountain volume, river network density, surface area, and surface roughness [13]. DEM can be applied in terrain and landform analysis, agricultural planting [14], land use [15], water resource utilization [16], environment and resource protection [17,18], urban construction and development [19,20], and other fields. The use of DEM can significantly promote efficiency and analytical development in various fields and provide accurate data to support social, natural, and applied science research.

Mountain Vertex is one component that can be derived using the DEM. For mountain ranges, a landform peak can be defined as a point with higher elevation than the adjacent areas. The shape is a geometric property of the peak on the arbitrarily selected surroundings (depending on the scale or level of detail) and is morphologically expressed as either being sharp, blunt, oblong, circular, conical, or other [21]. For this paper, mountain vertex extraction was based solely on DEM data in obtaining the highest peak values. As shown in Figure 1, the red point indicates the mountain vertex extracted from the raster DEM, while the blue point(s) shows the mountain peak(s) extracted from the same raster DEM. Some mountains may have one or more mountain peaks, but generally, most have only one mountain vertex.

One of DEM's most important applications is to define and characterize topographic features, in which the function of extraction of the mountain vertex is particularly useful. However, due to the influence of terrain changes, analysis scale, and other factors, mountain vertices extracted from the DEM can have inaccurate positions and incomplete information. In order to achieve rapid and efficient extraction of the mountain vertex, a number of methods have been proposed in the past few decades. These methods can be divided into two categories: (1) extraction methods that analyze local features of the mountain vertex [22–24], and (2) extraction methods that divide the spatial topography and geomorphology. For the first type of Mountain Vertex extraction methods, one study [25] used the Terrain Profile Analysis Method, which automatically extracted the maximum elevation value points in a local area through curve-fitting the horizontal (or vertical) section. However, this method was found to overlook key points and resulted in low accuracy. In another study [26], slope description factors and mathematical morphology were used to obtain the mountain vertex value. This method is also susceptible to missing points during processing, which could significantly affect the final results. At present, the most commonly used mountain vertex extraction is the Neighborhood Analysis-Comparison Method [27–29]. This approach constructs a sliding analysis window to obtain the maximum point of the current window by calculating the terrain feature factor. This is then used as a pre-selected point and is combined with the real mountain vertex areas to determine the required mountain vertices. However, this method has limited accuracy based on the size of the analysis window and requires eliminating relevant camouflage points.

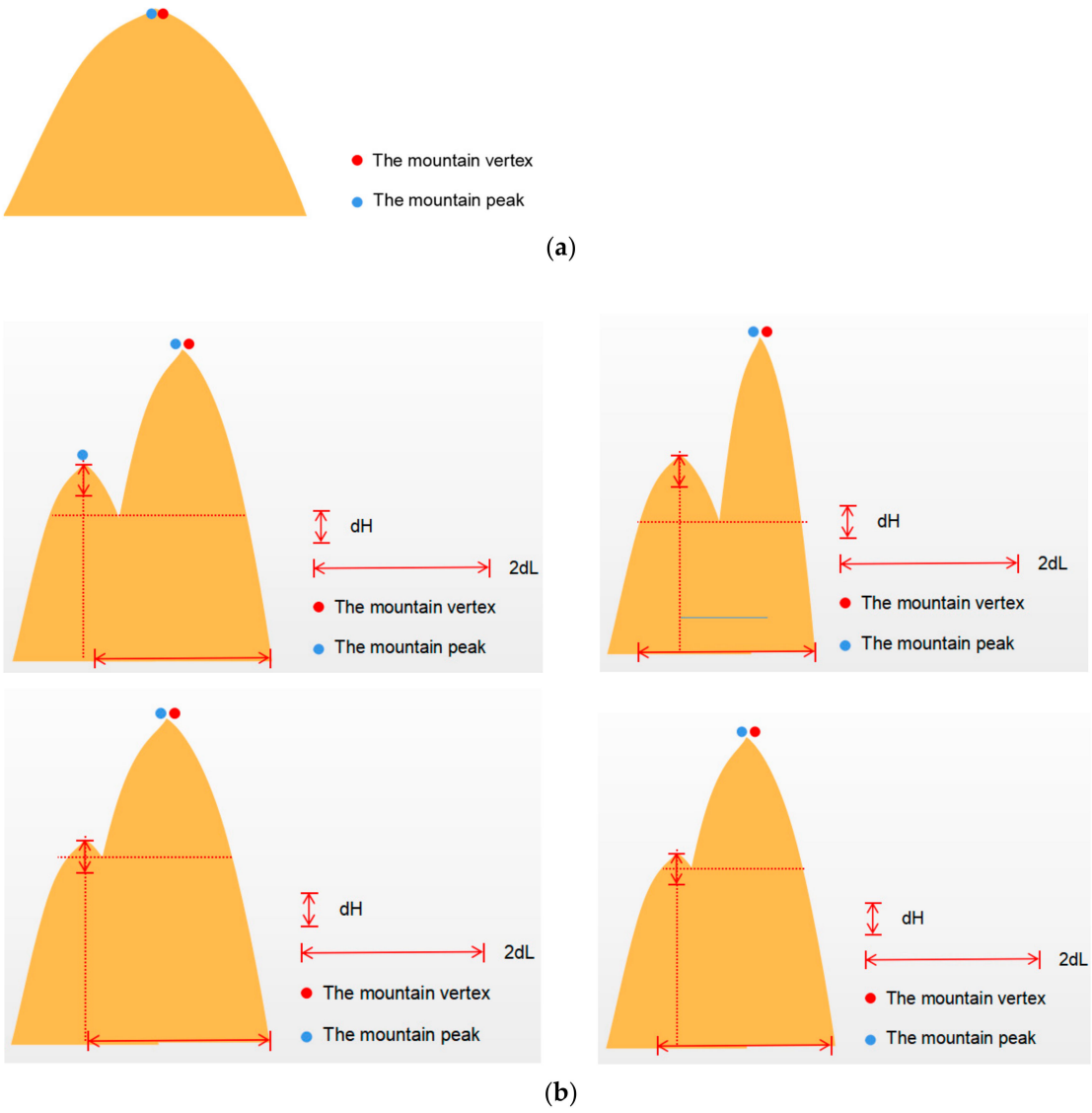

Figure 1. The difference between mountain vertex and the mountain peak. (**a**) A mountain with a single peak (the mountain vertex coincides with the mountain peak); (**b**) A mountain with two or multiple peaks (the mountain vertex is not always the same as the mountain peaks).

The second type of extraction method divides the spatial topography and geomorphology to obtain the mountain vertex and includes methods, such as the Hydrological Basin Extraction Method and the Contour Subdivision Method [30–34]. The Hydrological Basin Extraction Method [35] reverses the positive mountainous landform system, computes the flow direction to subdivide the watershed, and then calculates the grid to obtain the mountain vertex. Affected by the DEM interpolation, the fill-in threshold, the Watershed division calculation window, and other factors [36,37], this method does not identify erroneous mountain vertices and would therefore need to eliminate camouflage points. For the Contour Subdivision Method, contour lines are used to determine and interpolate the innermost mountain vertex area. One study [38] used contour lines and elevation values to characterize the terrain and constructed an analysis model, which was then used as a constraint to obtain the final results. Another study [39] proposed improvements based on the AKIMA Algorithm. The method improves the accuracy of the mountain vertex range interpolation and improves the extraction results. However, the Contour Line Division Method ignores the effects of adjacent mountains on the extraction results and are easily affected by topographical changes. Several methods have been proposed

that combine these two methods in order to improve the accuracy, such as the Water and Contour Division Overlay Method [40] and the Contour Line and Neighborhood Analysis Overlay Method.

In view of the problems of inaccurate mountain vertex extraction, this paper proposes a new approach that utilizes the Hotspot Analysis Clustering and Improved Eight-Connected Extraction algorithms to provide a quick and accurate determination of multiple mountain vertices for a given area. Our approach uses the elevation-based Hotspot Analysis Clustering to quickly divide the mountain vertex area, which effectively resolves the limitations of previous approaches. Compared with the Neighborhood Analysis Method, the Hotspot Analysis Clustering Algorithm can quickly divide the high- and low-value areas of the DEM required in mountain vertex extraction. The Algorithm can effectively reduce data produced by the Neighborhood Analysis Method and improve the processing efficiency of mountain vertex extraction. In contrast to the Neighborhood Analysis Method, the Hotspot Analysis Clustering Algorithm can minimize and even eliminate erroneous and false mountain vertices, particularly problematic for valleys, ridges, and areas with highly uneven terrain. Furthermore, the Hotspot Analysis Clustering Algorithm can significantly minimize errors in determining mountain vertex elevations, which is a major problem when using the Contour Line Method.

Our proposed approach also uses the Eight-Connected Extraction Algorithm to quickly determine the precise location and elevation of the vertices for multiple mountains in a given area. Compared with the Contour Line Method, the Eight-Connected Extraction Algorithm can provide more accurate results and balance the accuracy and efficiency of mountain vertex extraction. Seven datasets were used for the quantitative evaluation (Data 1, Data 2, Jianzhou New Town, Sichuan Province; Data 3, Data 4, Nanyang City, Henan Province; Data 5, Data 6, Ji'an City, Jiangxi Province; Data 7, Zhou'shan City, Zhejiang Province, China). The evaluation experiments were used to assess the efficiency and accuracy of the proposed approach in extracting mountain vertices compared to the other three methods. The results show that the proposed approach can quickly obtain the precise location and precise elevation value of multiple mountain vertices.

The remainder of this paper is organized as follows: Section 2 introduces the traditional mountain vertex Extraction methods and explains the Hotspot Analysis Clustering and Improved Eight-Connected Extraction Algorithms used in our proposed approach. Experiments and the discussion of results are provided in Section 3. The conclusions are presented in Section 4.

2. Methodology

2.1. Traditional Mountain Vertex Extraction Methods

The Contour Line Method extracts mountain vertices [39] by generating the contour lines from Raster DEM and uses the change range of the elevation variance to evaluate the vertex's influence range. It then finds the innermost contour line in the influence range and uses the interpolation algorithm to obtain the mountain vertex value. This method is affected by elevation and contour height difference threshold and generally yields low accuracy results of mountain vertices.

The Neighborhood Analysis Method extracts mountain vertices [27,28] by constructing an n × n analysis window and determines the maximum value within the window extent. The point is then used as a pre-selected point, which is then reclassified in order to obtain the mountain vertex. The main disadvantage of this method is that it is limited by the analysis window, which can generate more noise that needs to be cleared, thereby reducing efficiency.

The Contour Line and Neighborhood Analysis Overlay Methods [29] combines the two previous methods. The Contour Line Method is used to determine the area where the mountain vertex is located, while the Neighborhood Analysis Method acquires the pre-selected point. The results are then superimposed to obtain the mountain vertex. While

this method combines the two previously discussed methods, this approach still suffers similar constraints as those methods.

2.2. The Issues and Countermeasures Related to Traditional Mountain Vertex Extraction Methods

Traditional mountain vertex extraction methods are affected by the contour height difference threshold [39] and the analysis window set [27,28], leading to low accuracy results and more noise. Hotspot Analysis Clustering Algorithm can be used to minimize erroneous mountain vertices extracted using the Neighborhood Analysis Method and limit the mountain vertex area's range affected by the contour height difference threshold. Likewise, the Improved Eight-Connected Extraction Algorithm can improve the accuracy of mountain vertex extraction by the Contour Line Method and increase the efficiency of the Neighborhood Analysis Method. In this article, an algorithm is proposed that combines the Hotspot Analysis Clustering Algorithm and the Improved Eight-Connected Extraction Algorithm in order to quickly determine the precise location and elevation of multiple mountain vertices for a given area.

2.3. The Mountain Vertex Extraction Method Based on Hotspot Analysis Clustering and Improved Eight-Connected Extraction Algorithms

2.3.1. Basic Principles and Overall Technical Route

The pixel size is set after resampling to 10 × 10, and the original raster dataset is rotated by 45° and placed on top of the resampled Raster DEM. The nearest-neighbor interpolation algorithm is used to calculate the raster value for each resampled DEM image, and the original raster DEM is finally downsampled. The resampled DEM's boundary and spatial structure are then used to convert the DEM Data into a Point Vector dataset whose attributes are elevation values. The Getis-Ord Gi* Method is then used to calculate the point vector dataset, and the *p*-value and Z score of each point can be calculated. The hotspot (high elevation point) and cold-spot (low elevation point) can be defined based on the calculated *p*-value and Z-score. The DEM Hotspot Analysis Image Data is generated, which can then be used to define the DEM's high and low-value areas (i.e., DEM mountain vertex area extraction). Finally, the Improved Eight-Connected Extraction Algorithm is used to extract the accurate position and elevation of the mountain vertex from the DEM Hotspot Image Data (the high-value area and the low-value area division results of the DEM). The overall technical route is shown in Figure 2.

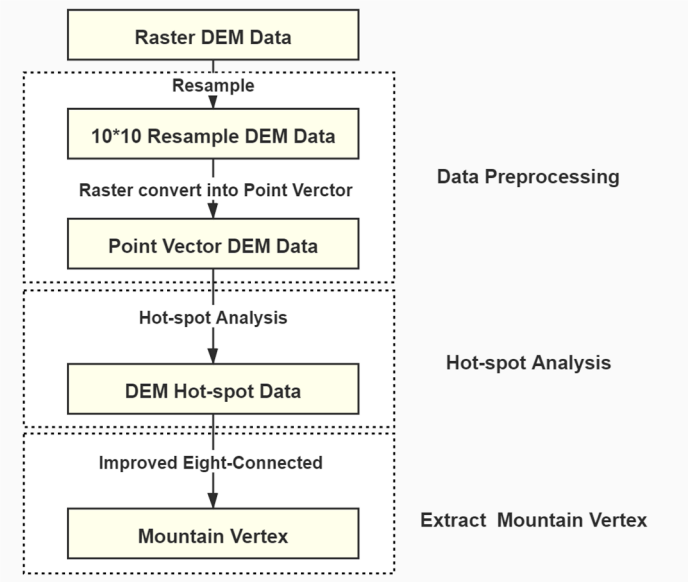

Figure 2. The overall technical route.

2.3.2. Data Preprocessing

DEM Data Resampling

The pixel size is set after resampling to 10 × 10. The original raster DEM is rotated by 45° and placed on top of the output resampled raster DEM. The nearest neighbor interpolation algorithm can be used to calculate the raster value for each resampling raster DEM. The cell value size in the new raster DEM is determined by the value of the nearest raster cell in the original DEM image. As shown in Figure 3, the blue points are the center of the raster cell of the original DEM, the green shaded area is the new raster DEM, the yellow shaded area is the area to be processed, and the red points are the cell centers of the new raster DEM. For each cell, the blue dots closest to the red dots are identified and marked in orange. The value of the orange point is used as the value of the red point.

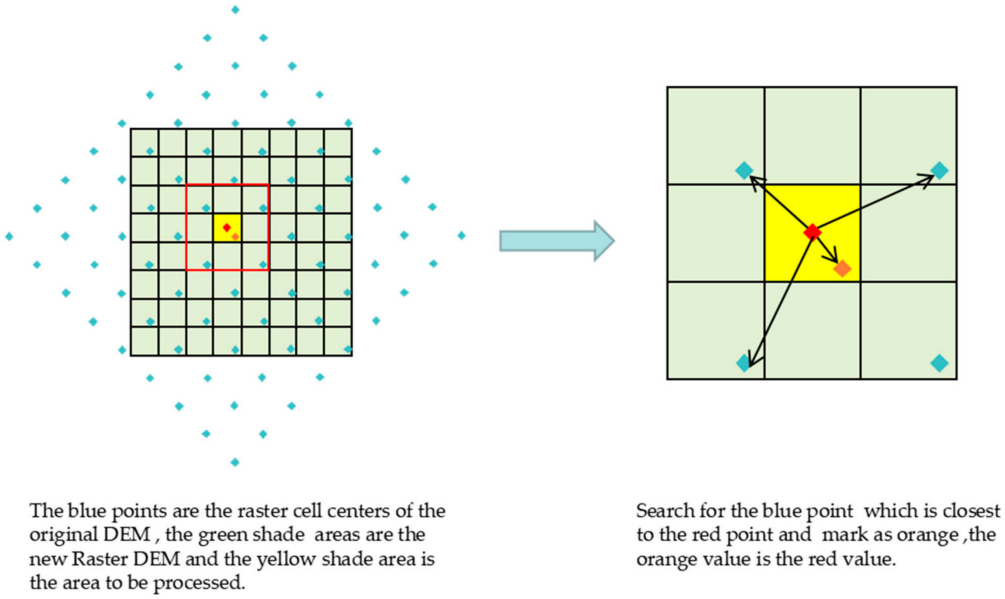

Figure 3. The resample processing of the Nearest Neighbor Interpolation Algorithm.

Using the above method, the raster DEM is converted into the resampled 10 × 10 pixel-size raster DEM.

Convert Raster DEM to Point Vector DEM

The resampled raster DEM is binarized to complete the extraction of the polygon boundary. The construction of the boundary arc is completed by searching each node from one to another. A complete topological structure and attribute connection can be formed based on its spatial relationship. Finally, redundant data caused by the search can then be removed. Through these operations, the Resampled Raster DEM is converted into a Point Vector DEM, and the attribute value for each point is based on the elevation from the DEM.

2.3.3. Extract the Mountain Vertices Region of DEM Based on the Hotspot Analysis Clustering Algorithm

Hotspot Analysis Clustering Algorithm

The Getis-Ord Gi* Method is an advanced version of the high-low value clustering [41], which can be used to calculate the point vector dataset. The *p*-value and Z score for each point can be obtained to define the hotspot (high elevation point) and cold-spot (low elevation point) and finish the high-low value clustering.

In analyzing the spatial correlation, the *p*-value represents the observed spatial pattern's probability being created by a random process. When the *p*-value is small and less than a certain threshold, this indicates that the spatial distribution is non-random and

follows a particular pattern [42]. The Z-score is a multiple of the standard deviation that mainly reflects the degree of dispersion of the dataset.

Both the *p*-value and the Z-score are related to the standard normal distribution, as shown in Figure 4.

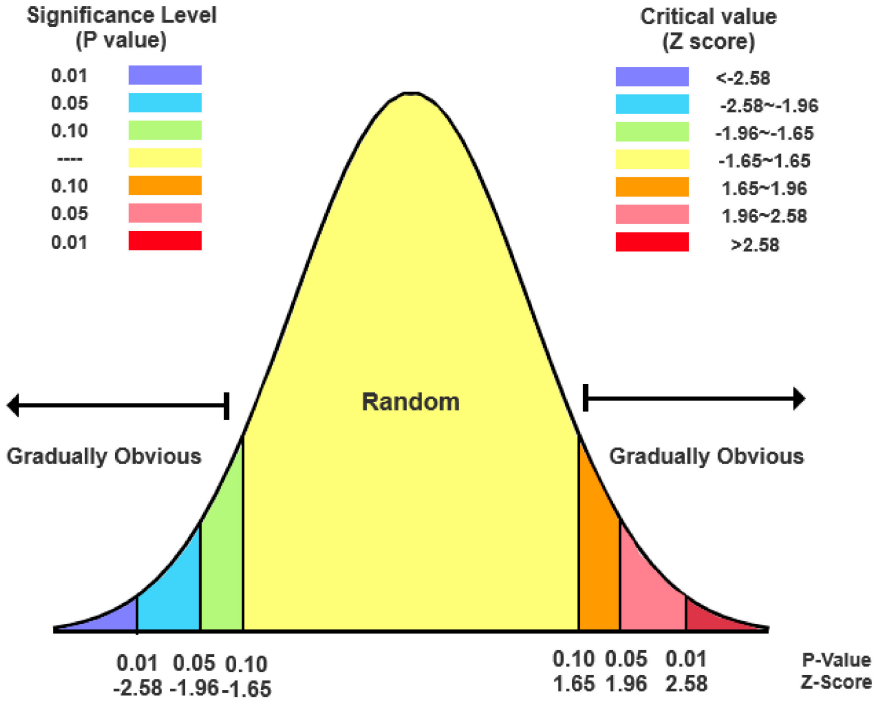

Figure 4. Normal distribution of *p*-value and Z-score.

The *p*-value and Z-score are correlated. Highly clustered and highly discrete data are both small probability events. If most of the calculated *p*-values and Z-scores are distributed on both sides, this would indicate that the probability of the spatial pattern being random is very low [41]. Confidence interval is used in estimating the overall parameter of the sample and is often associated with the *p*-value and Z-score, as shown in Table 1.

Table 1. The Correspondence between Z-score, *p*-value and the Confidence.

Z-Score	*p*-Value	Confidence
<−1.65 | | >+1.65	<0.10	90%
<−1.96 | | >+1.96	<0.05	95%
<−2.58 | | >+2.58	<0.01	99%

Using Equations (1)–(3), the Z-score (G_i^*) can be calculated for each element in the area.

$$G_i^* = \frac{\sum_{j=1}^{n} w_{i,j}x_j - \overline{X}\sum_{j=1}^{n} w_{i,j}}{S\sqrt{\frac{[n\sum_{j=1}^{n} w_{i,j}^2 - (\sum_{j=1}^{n} w_{i,j})^2]}{n-1}}} \quad (1)$$

where x_j is the attribute value of element j, and w_{ij} is the spatial weight between elements i and j (adjacent is 1, non-adjacent is 0), and n is the total number of elements [42].

$$\overline{X} = \frac{\sum_{j=1}^{n} x_j}{n} \quad (2)$$

$$S = \sqrt{\frac{\sum_{j=1}^{n} x_j^2}{n} - (\overline{X})^2} \quad (3)$$

Divide the High and Low-Value Region of the DEM Based on the Hotspot Analysis Clustering Algorithm

Using the Getis-Ord Gi* Method, Hotspot Analysis and Clustering were performed on the point vector DEM to define the hotspot (high elevation point) and cold-spot (low elevation point) based on the calculated *p*-value and Z-score. If the element's Z-score is high and the *p*-value is small, it means that there is high spatial clustering. If the element's Z-score is low (even negative) and the *p*-value is small, it means there is low spatial clustering. The higher (or lower) the Z-score, the greater (or lesser) the clustering degree. If the Z-score is close to zero, it means that there is no obvious spatial clustering. We can use the Z-score and *p*-value to obtain the location of the high-value (hotspot) or low-value (cold-spot) clustering to generate the Hotspot Analysis Image Data. The Z-score and *p*-value are statistical measures of hotspots and cold-spots used to judge whether to reject the null hypothesis on a factor-by-element basis [41–45].

The Hotspot Analysis Clustering Algorithm was then used to process the point vector DEM into the DEM Hotspot Analysis Image. The high-value regions (hotspot) were then extracted from the DEM Hotspot Analysis Image, where the Improved Eight-Connected Extraction Algorithm was employed to extract the mountain vertex.

2.3.4. Extract the Mountain Vertex Bases on the Improved Eight-Connected Extraction Algorithm

The Attribute Tag of the Point Vector DEM Hotspot Analysis Image Data

The attribute data of the DEM Hotspot Analysis Image was then exported. Using different *p*-value, Z-score, and confidence levels, numerical values (i.e., −3, −2, −1, 1, 2, 3 to 6) were assigned to the different situations. Table 2 summarizes the correspondence between the Z-score, *p*-value, confidence levels, and attribute H_Gi.

Table 2. The Correspondence between Z-score, *p*-value, Confidence, and the H_Gi value.

Z-Score	*p*-Value	Confidence	H_Gi
<−1.65 | | >+1.65	<0.10	90%	−1 | | 1
<−1.96 | | >+1.96	<0.05	95%	−2 | | 2
<−2.58 | | >+2.58	<0.01	99%	−3 | | 3

Improved Eight-Connected Extraction Algorithm

Eight-connectivity refers to the connection or link of a pixel in a given area towards any other pixel position using a combination of the eight directions (i.e., up, down, left, right, upper left, upper right, lower left, and lower right).

The Improved Eight-Connected Extraction algorithm mainly improves the eight-direction into four-way optimization. First, the attribute value in four directions (left, upper left, upper, and right) is evaluated on whether it is the desired attribute and assessed for its connectivity. If the answer is yes, the cell is marked. As shown in Figure 5, since the attribute values on the cells to the left, upper left, upper, and right sides of point A are consistent, the cell is marked accordingly.

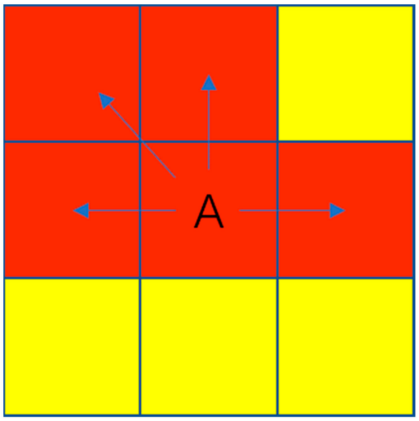

Figure 5. The four-way optimization labeled graph of the Improved Eight-Connected Extraction Algorithm.

After the first marking is completed, the image undergoes a second assessment process and is scanned from left to right and top to bottom to find the marked point. Each marked cell is reevaluated to determine whether the attribute value is the same at the four other direction points (i.e., upper right, lower right, lower left, and bottom). If so, the final mark will be carried out [45–47]. As shown in Figure 6, both A and B meet the four-way optimization requirements and are marked accordingly. After all the cells are marked for the first time, the marked points undergo the second assessment procedure. In the example, only point A meets the requirement and is marked accordingly. On the other hand, Point B does not meet the second screening procedure, which means no further processing will be done on the cell.

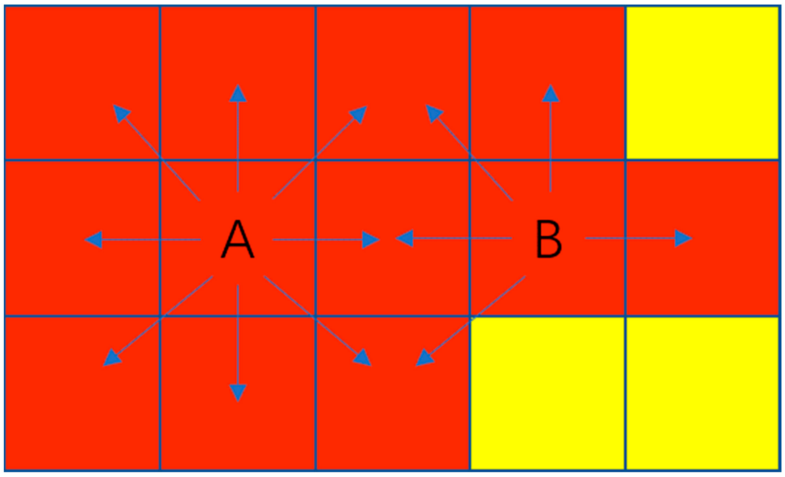

Figure 6. The diagram of secondary Marking Method.

Mountain Vertex Extraction Based on the Improved Eight-Connected Extraction Algorithm

The Improved Eight-Connected Algorithm is used to mark the points with the H_Gi attribute value of 3 (Z-score > +2.58, *p*-value < 0.01) in the DEM Hotspot Analysis Image (shown in red in Figure 7). The marked points are represented as blue cells in the image. After the marking procedure is completed, the image is scanned from left to right and top to bottom. The points are then grouped according to whether they are adjacent to other marked points. As shown in the figure, points A, B, C, D, and E are grouped together, while points F, G, H, and I are clustered in another group. The cell with the highest elevation attribute in each group is then considered as the candidate mountain vertex.

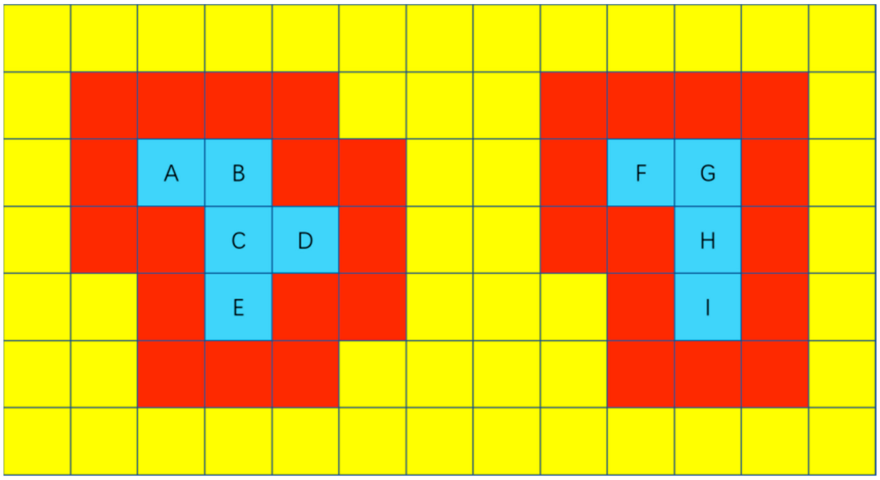

Figure 7. Schematic diagram of mountain vertex extraction based on the Improved Eight-Connected Extraction Algorithm.

The highest elevation point among the candidate peaks is the mountain vertex. If two or more cells have the highest elevation value in a given group area, they are all considered the mountain vertices.

3. Experiments and Results

3.1. Experimental Setup

In this paper, we used an I7-8700 CPU, 16G RAM, and RTX2080 GPU computer to conduct the experimental tests on seven sets of raster DEM data from different experimental areas or mountain types (as shown in Table 3).

Table 3. The difference between the experimental data.

NO.	Data Location	Data Range	Data Type	Spatial Resolution	Data Height
1	Jianzhou	104.10°E–104.16°E 30.60°N~30.66°N	Raster	1 m	high mountain: 429 m~483 m
2	Jianzhou	104.10°E~104.19°E 30.59°N~30.64°N	Raster	1 m	high mountain: 430 m~485 m
3	Nanyang	112.06°E–112.08°E 33.185°N~30.20°N	Raster	2 m	middle mountain: 231 m~277 m
4	Nanyang	112.06°E–112.07°E 33.12°N~30.16°N	Raster	2 m	middle mountain: 237 m~280 m
5	Ji'an	114.23°E–114.236°E 27.19°N~27.20°N	Raster	2 m	low mountain: 66 m~105 m
6	Ji'an	114.11°E–114.12°E 27.18°N~27.19°N	Raster	2 m	low mountain: 59 m~106 m
7	Zhou'shan	122.03°E–122.16°E 30.06°N~30.16°N	Raster	2 m	high mountain: −888 m~522 m

In this paper, we used the reference method to extract the mountain vertex for Datasets 1 to 7, which are then used as the reference data to be compared with the results from other methods. The reference method uses the contour line method to divide the mountain area and sort the elevation values to get the highest point of the mountain. The highest point for each mountain serves as the mountain vertex. The proposed approach, which uses the Hotspot Analysis and Improved Eight-Connected Extraction algorithms, was used to extract mountain vertices for Datasets 1 to 7. For comparative analysis, the Contour Line

Method with a 3 m-contour interval, the Neighborhood Analysis Method with 6 × 6 control window, and the Contour Line and Neighborhood Analysis Overlay Method with 3 m contour interval of and 6 × 6 control window were employed separately in extracting mountain vertices [30,48]. The extraction results were then compared in terms of the number of mountain vertices identified, the extraction rate, the accuracy rate, and the time used by each method. These experimental results were then compared and were used in evaluating the pros and cons of each method.

3.2. The First Dataset: The Northern Part of the West Area of the Jianzhou New Town, China

3.2.1. Experimental Data Description

The first dataset consists of a raster DEM of Jianzhou New Town, Sichuan Province, China (longitude: 104.10°E–104.16°E, latitude: 30.60°N~30.66°N). As shown in Figure 8, the image has a 1 m spatial resolution, uses the CGCS2000 coordinate system, and has 610 rows and 690 columns. The terrain is mainly mountainous, with an average altitude of 429~483 m and a height difference of about 54 m. Figure 8 shows the data and results for Dataset 1: (a) is the Digital Orthophoto Map (DOM), (b) is the Digital Elevation Model (DEM), and (c) is the hillshading results.

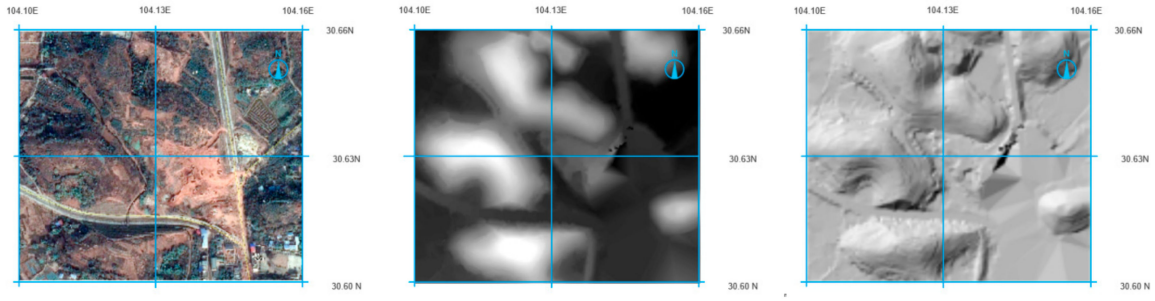

(**a**) DOM data of the first dataset (the northern part of Jianzhou, China)

(**b**) DEM data of the first dataset (the northern part of Jianzhou, China)

(**c**) Hillshading result of the first dataset (the northern part of Jianzhou, China)

Figure 8. Experimental results for Dataset 1: (**a**) DOM data for Dataset 1 (Jianzhou); (**b**) DEM data for Dataset 1 (Jianzhou); (**c**) Hillshading results for Dataset 1 (Jianzhou).

3.2.2. Comparison of the Mountain Vertex Extraction Results for the First Dataset

The proposed approach and conventional extraction methods were used and compared in extracting the mountain vertices for the first dataset. The distribution graphs of vertices extracted by each method are shown in the succeeding figures. Figure 9 presents the accurate mountain vertex distribution map extracted using the reference method. Figure 10 shows the distribution maps generated using conventional extraction methods: Figure 10a using the Contour Line Extraction Technique, Figure 10b using the Neighborhood Analysis Method, and Figure 10c using the Contour Line and Neighborhood Analysis Overlay Method. Figure 11 displays the generated distribution map from our proposed approach that uses Hotspot Analysis and Improved Eight-Connected Extraction Algorithms in extracting mountain vertices.

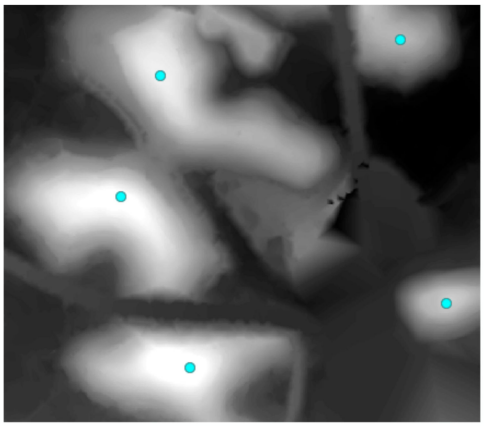

Figure 9. The distribution map of the experimental first dataset extracted using the reference method.

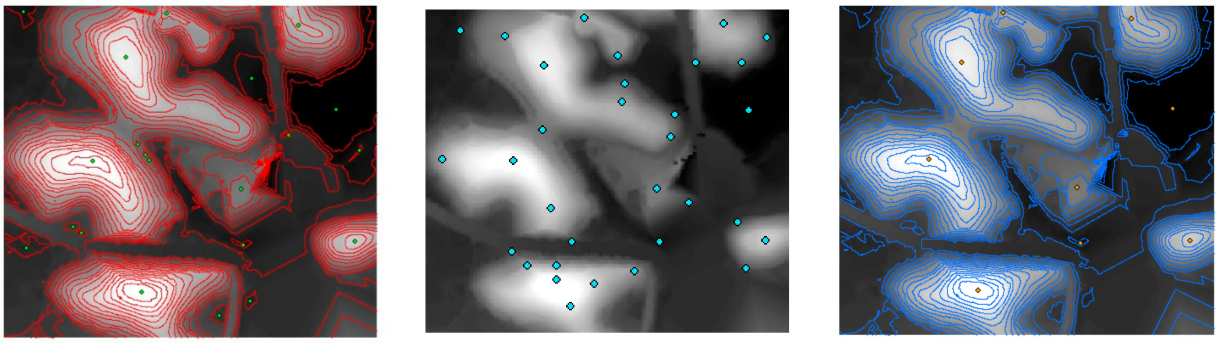

(**a**) (**b**) (**c**)

Figure 10. The experimental first dataset distribution map extracted using traditional mountain vertex extraction methods: (**a**) Contour Line Method; (**b**) Neighborhood Analysis Method; and (**c**) Contour line and Neighborhood Analysis Overlay Method.

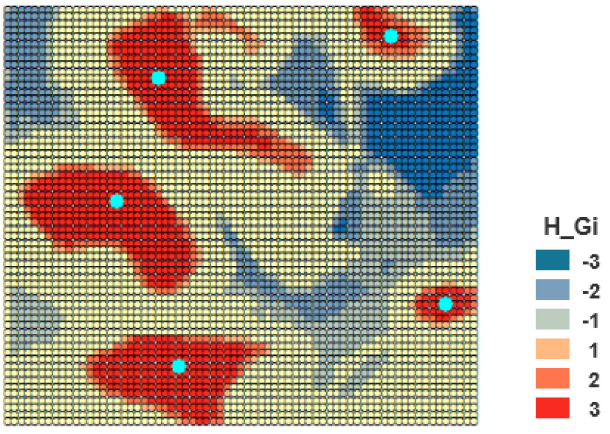

Figure 11. The distribution map for the first dataset using our proposed approach.

The extraction results generated by the different methods were then sorted, tabulated, and compared in terms of extraction rate and accuracy. The summary of results is presented in Table 4.

Table 4. Vertex extraction results for each method using the experimental first dataset.

Method	Extract NUM	Correct NUM	False NUM	Extract Rate	Correct Rate
Reference Method	5	5	0	100%	100%
The Proposed Method	5	5	0	100%	100%
CLM	21	3	2	14%	60%
NAM	32	4	1	12.5%	80%
CLaNAOM	9	4	1	45%	80%

As shown in Table 4, the Reference Method, the Proposed Method, the Contour Line Method, the Neighborhood Analysis Method, and the Contour Line and Neighborhood Analysis Overlay Method were used to process the first dataset. The number of the mountain vertices extracted were 5, 5, 21, 32, 9, and the accuracy rate was 100%, 100%, 14%, 12.5%, and 45%. The experimental results show that the Reference Method and the Proposed Method performed considerably better.

3.2.3. Comparison of the Mountain Vertex Extraction Time for the First Dataset

The time expended in extracting mountain vertices using our proposed approach and using the Contour Line and Neighborhood Analysis Overlay Method were recorded and compared. Table 5 presents the summary of time consume results using our proposed approach, and Table 6 tabulates the summary of time consume results using the Contour Line and Neighborhood Analysis Overlay Method.

Table 5. The time consumed in extracting mountain vertices for the first dataset using our proposed approach.

NO.	Method	Time
1	Resampling of the raster DEM by 10 × 10 pixel-size	1.5 s
2	Raster DEM conversion into point vector DEM	1.5 s
3	Hotspot analysis of the point vector DEM	3 s
4	Extraction of mountain vertices	4 s
	Total Time	**10 s**

Table 6. The time spent in extracting mountain vertices for the first dataset using the Contour Line and Neighborhood Analysis Overlay Method.

NO.	Method	Time
1	Set 6 × 6 analysis window to neighborhood analyze the Raster DEM image data	6 s
2	Generate 3 m interval contour lines for DEM images, extract the innermost contour line area	5.5 s
3	Calculate the intersection between the innermost circle of DEM and the neighborhood analysis obtain data to get the experimental first dataset's Mountain Vertices	3.5 s
	Total Time	**15 s**

The proposed method (the 10 × 10 resampling size) and the Contour Line and the Neighborhood Analysis Overlay Method (the 6 × 6 analysis window, the 3-m contour interval) were then used to extract the mountain vertices for Dataset 1. The experimental results for Dataset 1 show that the proposed method performed 1.5 times faster than the Contour Line and Neighborhood Analysis Overlay Method.

3.3. The Second Dataset: The Lower Part of the South Area of the Jianzhou New Town, China

3.3.1. Experimental Data Description

The experimental second dataset (see Figure 12) consists of a Raster DEM Image in Jianzhou, Sichuan Province (longitude: 104.10°E~104.19°E, latitude: 30.59°N~30.64°N). Similar to Dataset 1, the image has a 1-m spatial resolution, uses the CGCS2000 coordinate system, and has 455 rows and 968 columns. The second dataset has a general high mountain topography, with an average altitude of 430~485 m and a height difference of about 55 m. Figure 12 shows the data and results for Dataset 2: (a) is the Digital Orthophoto Map (DOM), (b) is the Digital Elevation Model (DEM), and (c) is the hillshading results.

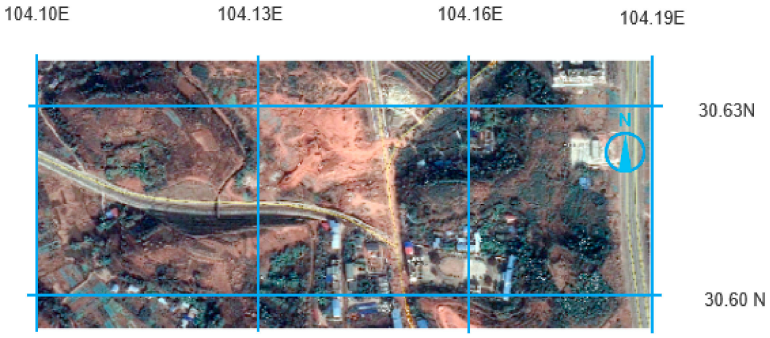

(**a**) DOM data of the second dataset (the southern part of Jianzhou, China)

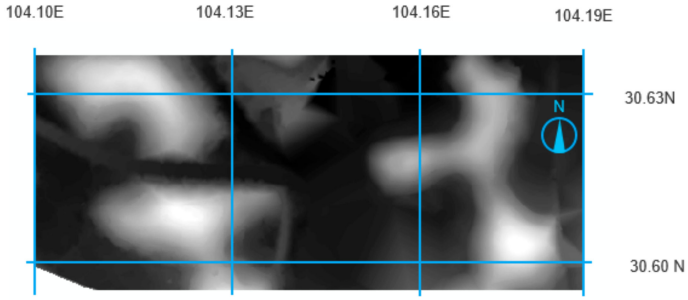

(**b**) DEM data of the second dataset (the southern part of Jianzhou, China)

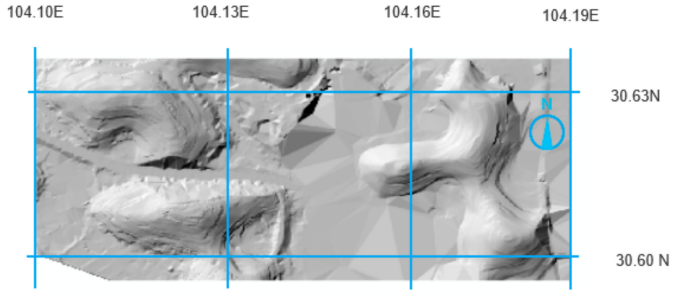

(**c**) Hillshading result of the second dataset (the southern part of Jianzhou, China)

Figure 12. The experimental second dataset: (**a**) DOM data of the second dataset (Jianzhou); (**b**) DEM data of the second dataset (Jianzhou); (**c**) Hillshading result of the second dataset (Jianzhou).

3.3.2. Comparison of the Mountain Vertex Extraction Results for the Second Dataset

The second dataset was also used to compare the different methods of mountain vertex extraction. The distribution graphs of Mountain Vertices extracted by each method are shown in the following figure. Figure 13 shows the accurate mountain vertex distribution map extracted using the reference method. Figure 14a shows the distribution map using the Contour Line Extraction procedure, Figure 14b using the Neighborhood Analysis Method, and Figure 14c using the Contour Line and Neighborhood Analysis Overlay Method. The

distribution map of mountain vertices extracted using our proposed approach is provided in Figure 15.

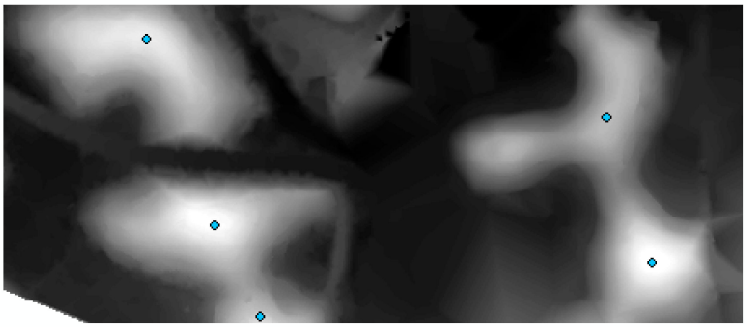

Figure 13. The distribution map of the second dataset extracted using the reference method.

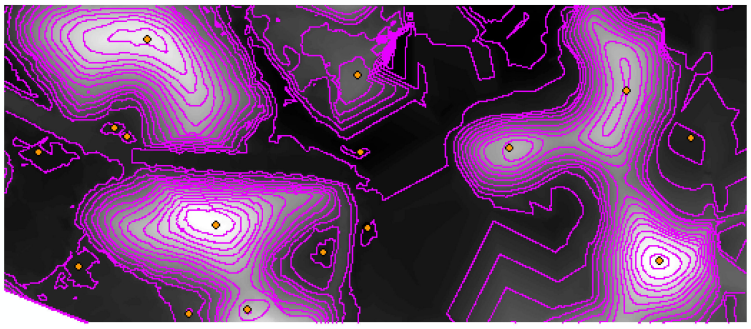

(**a**)

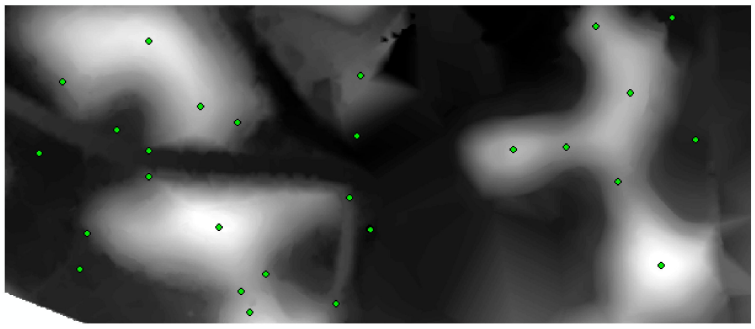

(**b**)

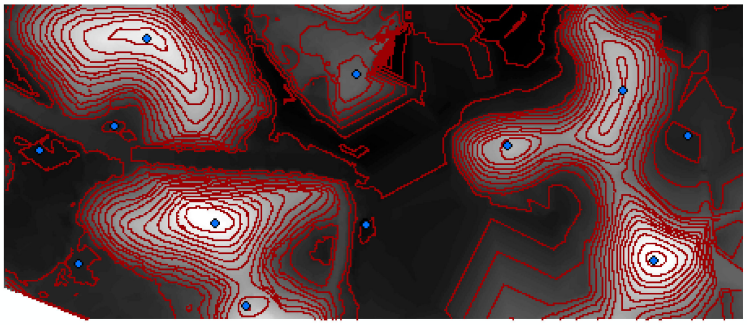

(**c**)

Figure 14. Distribution maps extracted by the traditional Mountain Vertices Extraction Methods using the second dataset. (**a**) Contour Line Method. (**b**) Neighborhood Analysis Method. (**c**) Contour line and Neighborhood Analysis Overlay Method.

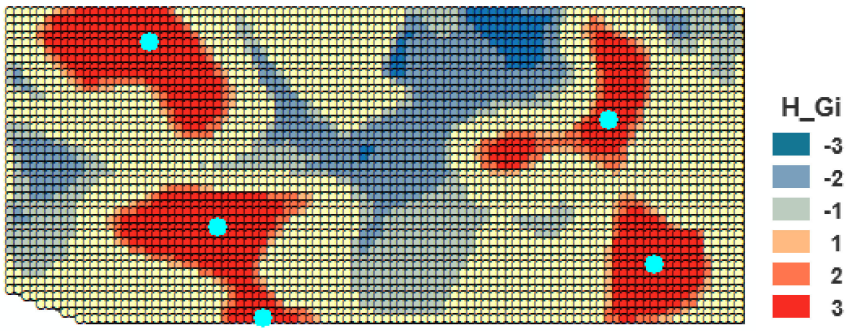

Figure 15. The distribution map for the second dataset using our proposed approach.

The extraction results using the different mountain vertex extraction methods were evaluated in terms of the extraction rate the resulting accuracy. The summary of results is provided in Table 7.

Table 7. The mountain vertices extraction results for each method using the second dataset.

Method	Extract NUM	Correct NUM	False NUM	Extract Rate	Correct Rate
Reference Method	5	5	0	100%	100%
The Proposed Method	5	5	0	100%	100%
CLM	16	3	2	19%	60%
NAM	27	4	1	15%	80%
CLaNAOM	12	4	1	33%	80%

As shown in Table 7, the Reference Method, the Proposed Method, the Contour Line Method, the Neighborhood Analysis Method, and the Contour Line and Neighborhood Analysis Overlay Method were used to process the second dataset. The mountain vertices extracted were 5, 5, 16, 27, and 12, and the accuracy rate is 100%, 100%, 19%, 15%, and 33%. The experiment shows that the Reference Method and the Proposed Method had significantly better results.

3.3.3. Comparison of the Mountain Vertex Extraction Time Using Experimental Second Dataset

The time expended in extracting mountain vertices for the second dataset using our proposed approach and using the Contour Line and Neighborhood Analysis Overlay Method were recorded and compared. Table 8 shows the time consumed in extracting mountain vertices for the second dataset using our proposed approach, while Table 9 shows time results using the Contour Line and Neighborhood Analysis Overlay Method.

Table 8. The time consumed in extracting mountain vertices for the second dataset using our proposed approach.

NO.	Method	Time
1	Resampling of the Raster DEM by 10 × 10 pixel-size	1.1 s
2	Raster DEM conversion into point vector DEM	1.2 s
3	Hotspot analysis of the Point Vector DEM	2.7 s
4	Extraction of the mountain vertices	3.6 s
	Total Time	**8.6 s**

Table 9. The time spent in extracting mountain vertices for the second dataset using the Contour Line and Neighborhood Analysis Overlay Method.

NO.	Method	Time
1	Set 6 × 6 analysis window to neighborhood analyze the Raster DEM image data	5.3 s
2	Generate 3 m interval contour lines for DEM images, extract the innermost contour line area	4.9 s
3	Calculate the intersection between the innermost circle of DEM and the neighborhood analysis obtain data to get the experimental second dataset's Mountain Vertices	3 s
	Total Time	**13.2 s**

The proposed method (the 10 × 10 resampling size) and the Contour Line and the Neighborhood Analysis Overlay Method (the 6 × 6 analysis window, the 3-m contour interval) were then used to extract the mountain vertices for Dataset 2. The proposed method was 1.5 times faster than the Contour Line and Neighborhood Analysis Overlay Method for Dataset 2.

3.4. The Third Dataset: The Northern Region of the West Area of the Nanyang, China

3.4.1. Experimental Data Description

The third dataset consists of a Raster DEM of Nanyang City, Henan Province, China (longitude: 112.06°E–112.08°E, latitude: 33.185°N~30.20°N). As shown in Figure 16, the image has a 2 m spatial resolution, uses the CGCS2000 coordinate system, and has 176 rows and 236 columns. The terrain has medium-sized mountains, with an average altitude of 231~277 m and a height difference of about 43 m. Figure 17 shows the data and results for Dataset 3: (a) is the Digital Orthophoto Map (DOM), (b) is the Digital Elevation Model (DEM), and (c) is the hillshading results.

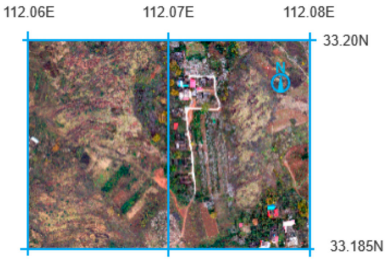

(**a**) DOM data of the third dataset (the northern part of Nanyang, China)

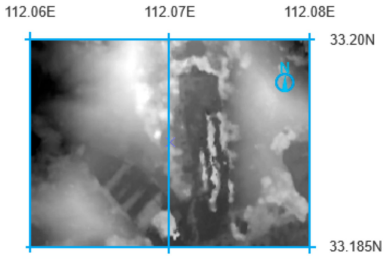

(**b**) DOM data of the third dataset (the northern part of Nanyang, China)

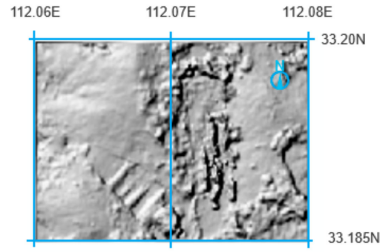

(**c**) Hillshading result of the third dataset (the northern part of Nanyang, China)

Figure 16. The third dataset: (**a**) DOM data of the third dataset (the northern part of Nanyang, China); (**b**) DEM data of the third dataset (the northern part of Nanyang, China); (**c**) Hillshading result of the third dataset (the northern part of Nanyang, China).

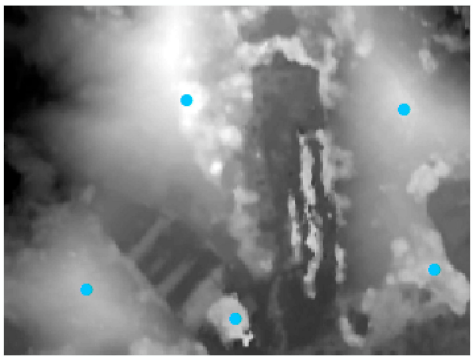

Figure 17. The distribution map of the third dataset extracted using the reference method.

3.4.2. Comparison of the Mountain Vertex Extraction Results for the Third Dataset

The third dataset was also used to compare the different methods of mountain vertex extraction. The distribution graphs of the mountain vertices extracted by each method are shown in the succeeding figures. Figure 17 shows the accurate mountain vertex distribution map extracted using the reference method. Figure 18a shows the distribution map using the Contour Line Extraction procedure, Figure 18b using the Neighborhood Analysis Method, and Figure 18c using the Contour Line and Neighborhood Analysis Overlay Method. The distribution map for the mountain vertices extracted using our proposed approach is provided in Figure 19.

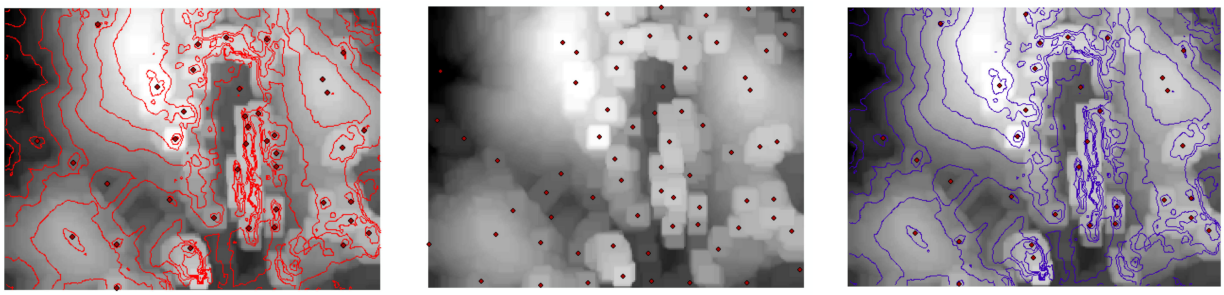

(**a**) (**b**) (**c**)

Figure 18. Distribution maps extracted by the traditional Mountain Vertices Extraction Methods using the third dataset. (**a**) Contour Line Method. (**b**) Neighborhood Analysis Method. (**c**) Contour line and Neighborhood Analysis Overlay Method.

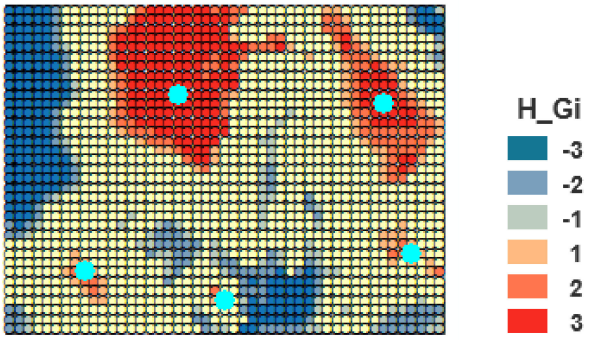

Figure 19. The distribution map for the third dataset using our proposed approach.

The extraction results using the different mountain vertex extraction methods were evaluated in terms of the extraction rate the resulting accuracy. The summary of results is provided in Table 10.

Table 10. The mountain vertices extraction results for each method using the third dataset.

Method	Extract NUM	Correct NUM	False NUM	Extract Rate	Correct Rate
Reference Method	5	5	0	100%	100%
The Proposed Method	5	5	0	100%	100%
CLM	41	3	2	7.3%	60%
NAM	63	4	1	6.3%	80%
CLaNAOM	34	4	1	11.8%	80%

As presented in Table 10, the Reference Method, the Proposed Method, the Contour Line Method, the Neighborhood Analysis Method, and the Contour Line and Neighborhood Analysis Overlay Method were used to process the third dataset. The mountain vertices extracted were 5, 5, 41, 63, and 34, and the accuracy rates are 100%, 100%, 7.3%, 6.3%, and 11.8%. The experimental results show that the Reference Method and the Proposed Method are significantly better.

3.4.3. Comparison of the Mountain Vertex Extraction Time Using Experimental the Third Dataset

The time spent extracting the mountain vertices for the third dataset using our proposed approach and using the Contour Line and Neighborhood Analysis Overlay Method were recorded and compared. Table 11 shows the vertex extraction time for the third dataset using our proposed approach, while Table 12 shows the results using the Contour Line and Neighborhood Analysis Overlay Method.

Table 11. The time consumed in extracting mountain vertices for the third dataset using our proposed approach.

NO.	Method	Time
1	Resampling of the Raster DEM by 10 × 10 pixel-size	0.21 s
2	Raster DEM conversion into point vector DEM	0.26 s
3	Hotspot analysis of the Point Vector DEM	0.33 s
4	Extraction of the mountain vertices	0.45 s
	Total Time	**1.25 s**

Table 12. The time spent in extracting mountain vertices for the third dataset using the Contour Line and Neighborhood Analysis Overlay Method.

NO.	Method	Time
1	Set 6 × 6 analysis window to neighborhood analyze the Raster DEM data	0.59 s
2	Generate 3 m interval contour lines for DEM data, extract the innermost contour line area	0.54 s
3	Calculate the intersection between the innermost circle of DEM and the neighborhood analysis obtain data to get the experimental third dataset's Mountain Vertices	0.34 s
	Total Time	**1.47 s**

The proposed method (the 10 × 10 resampling size) and the Contour Line and the Neighborhood Analysis Overlay Method (the 6 × 6 analysis window, the 3 m contour interval) were used to extract the mountain vertices for Dataset 3. For Dataset 3, the proposed Method was 1.2 times faster than the Contour Line and Neighborhood Analysis Overlay Method.

3.5. The Fourth Dataset: The Southern Region of the West Area of Nanyang, China

3.5.1. Experimental Data Description

The fourth dataset consists of a Raster DEM of Nanyang City, Henan Province, China (longitude: 112.06°E–112.07°E, latitude: 33.12°N~30.16°N). As shown in Figure 20, the image has a 2 m spatial resolution, uses the CGCS2000 coordinate system, and has 261 rows and 166 columns. The terrain has medium-sized mountains, with an average altitude of 237~280 m and a height difference of about 43 m. Figure 20 shows the data and results for Dataset 4: (a) is the Digital Orthophoto Map (DOM), (b) is the Digital Elevation Model (DEM), and (c) is the hillshading results.

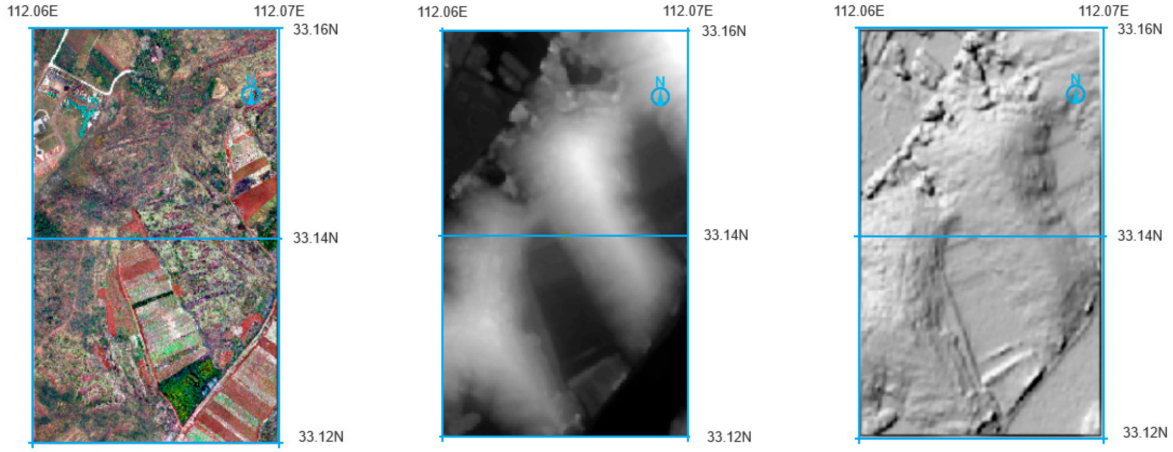

(**a**) DOM data of the fourth dataset (the southern part of Nanyang, China)

(**b**) DEM data of the fourth dataset (the southern part of Nanyang, China)

(**c**) Hillshading result of the fourth Dataset (the southern part of Nanyang, China)

Figure 20. The fourth dataset: (**a**) DOM data of the fourth dataset (the southern part of Nanyang, China); (**b**) DEM data of the fourth dataset (the southern part of Nanyang, China); (**c**) Hillshading result of the fourth dataset (the southern part of the Nanyang, China).

3.5.2. Comparison of the Mountain Vertex Extraction Results for the Fourth Dataset

The fourth dataset was also used to compare the different methods of mountain vertex extraction. The distribution graphs of mountain vertices extracted by each method are shown in the succeeding figures. Figure 21 shows the accurate mountain vertex distribution map extracted using the Reference Method. Figure 22a shows the distribution map using the Contour Line Extraction procedure, Figure 22b using the Neighborhood Analysis Method, and Figure 22c using the Contour Line and Neighborhood Analysis Overlay Method. The distribution map of mountain vertices extracted using our proposed approach is provided in Figure 23.

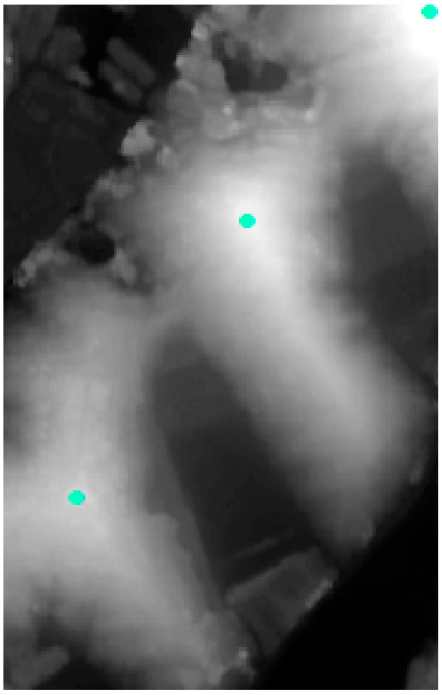

Figure 21. The distribution map of the fourth dataset extracted using the reference method.

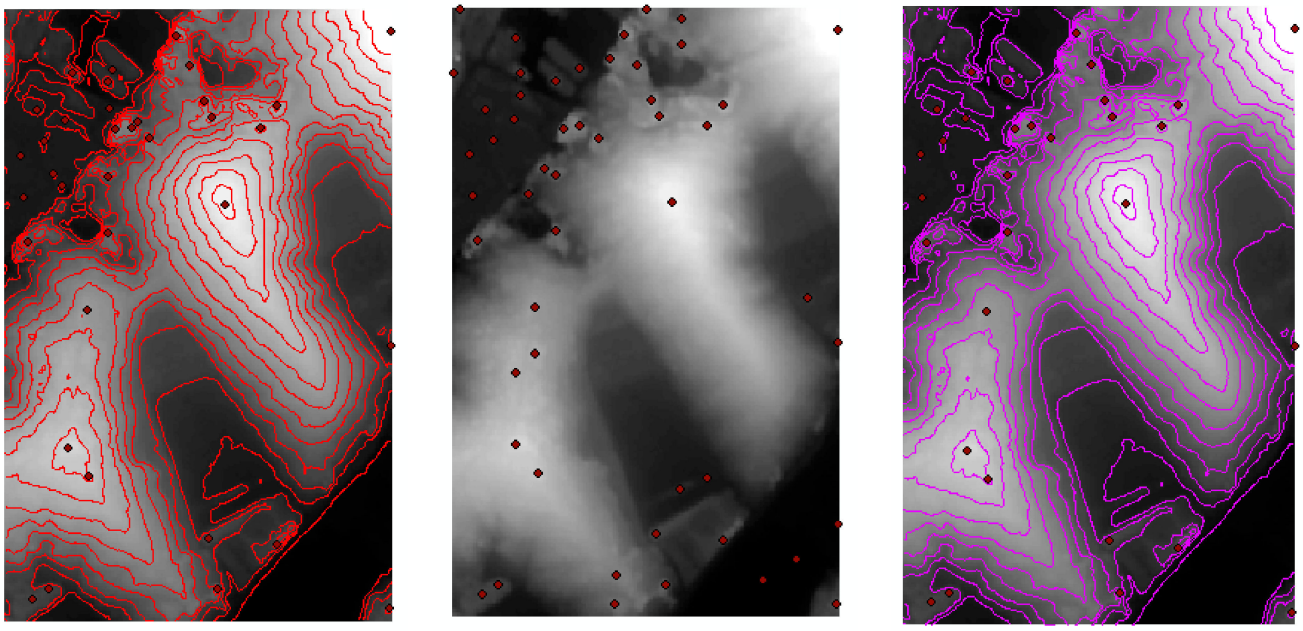

(**a**) (**b**) (**c**)

Figure 22. Distribution maps extracted by the traditional Mountain Vertices Extraction Methods using the fourth dataset. (**a**) Contour Line Method. (**b**) Neighborhood Analysis Method. (**c**) Contour line and Neighborhood Analysis Overlay Method.

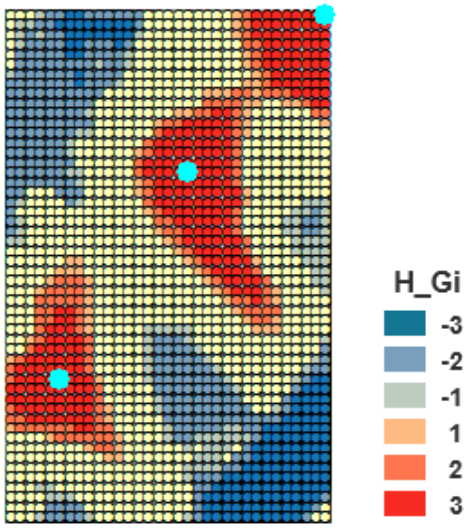

Figure 23. The distribution map for the fourth dataset using our proposed approach.

The extraction results using the different mountain vertex extraction methods were evaluated in terms of the extraction accuracy rates. The summary of results is provided in Table 13.

Table 13. The mountain vertices extraction results for each method using the fourth dataset.

Method	Extract NUM	Correct NUM	False NUM	Extract Rate	Correct Rate
Reference Method	3	3	0	100%	100%
The Proposed Method	3	3	0	100%	100%
CLM	33	2	1	6%	80%
NAM	47	2	1	4.3%	80%
CLaNAOM	27	2	1	7.4%	80%

The Reference Method, the Proposed Method, the Contour Line Method, the Neighborhood Analysis Method, and the Contour Line and Neighborhood Analysis Overlay Method were used to process the fourth dataset. Table 13 shows the summary of extraction results. The number of extracted mountain vertices are 3, 3, 33, 47, and 27, and the accuracy rates are 100%, 100%, 6%, 4.3%, and 7.4%. The experimental results show that the Reference Method and the Proposed Method performed much better.

3.5.3. Comparison of the Mountain Vertex Extraction Time Using the Fourth Dataset

The time expended in extracting mountain vertices for the fourth dataset using our proposed approach and using the Contour Line and Neighborhood Analysis Overlay Method were recorded and compared. Table 14 shows the time consumed in extracting mountain vertices for the fourth dataset using our proposed approach, while Table 15 shows time results using the Contour Line and Neighborhood Analysis Overlay Method.

Table 14. The time consumed in extracting mountain vertices for the fourth dataset using our proposed approach.

NO.	Method	Time
1	Resampling of the Raster DEM by 10 × 10 pixel-size	0.23 s
2	Raster DEM conversion into point vector DEM	0.29 s
3	Hotspot analysis of the Point Vector DEM	0.36 s
4	Extraction of the mountain vertices	0.50 s
	Total Time	**1.38 s**

Table 15. The time spent in extracting mountain vertices for the fourth dataset using the Contour Line and Neighborhood Analysis Overlay Method.

NO.	Method	Time
1	Set 6 × 6 analysis window to neighborhood analyze the Raster DEM data	0.65 s
2	Generate 3 m interval contour lines for DEM data, extract the innermost contour line area	0.59 s
3	Calculate the intersection between the innermost circle of DEM and the neighborhood analysis obtain data to get the experimental fourth dataset's Mountain Vertices	0.37 s
	Total Time	**1.61 s**

For Dataset 4, the proposed method (the 10 × 10 resampling size) and the Contour Line and the Neighborhood Analysis Overlay Method (the 6 × 6 analysis window the 3-m contour interval) were used in extracting the mountain vertices. The experimental results show that the proposed method was 1.2 times faster than the Contour Line and Neighborhood Analysis Overlay Method for Dataset 4.

3.6. The Fifth Dataset: The Eastern Portion of the West Area of the Ji'an, China

3.6.1. Experimental Data Description

The fifth dataset consists of a raster DEM of Ji'an City, Jiangxi Province, China ((longitude: 114.23°E–114.236°E, latitude: 27.19°N~27.20°N). As shown in Figure 24, the image has a 2 m spatial resolution, uses the CGCS2000 coordinate system, and has 132 rows and 111 columns. The terrain has low mountains, with an average altitude of 66–105 m and a height difference of about 39 m. Figure 24 shows the data and results for Dataset 5: (a) is the Digital Orthophoto Map (DOM), (b) is the Digital Elevation Model (DEM), and (c) is the hillshading results.

(**a**) DOM data of the fifth dataset (the eastern part of Ji'an, China)

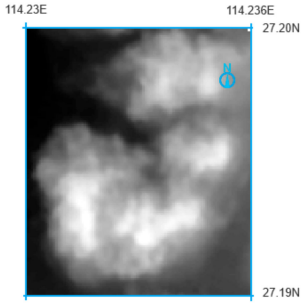

(**b**) DEM data of the fifth dataset (the eastern part of Ji'an, China)

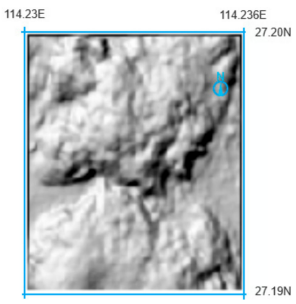

(**c**) Hillshading result of the fifth dataset (the eastern part of Ji'an, China)

Figure 24. The experimental fifth dataset: (**a**) DOM data of the fifth dataset (the eastern part of Ji'an, China); (**b**) DEM data of the fifth dataset (the eastern part of Ji'an, China); (**c**) hillshading result of the fifth dataset (the eastern part of Ji'an, China).

3.6.2. Comparison of the Mountain Vertex Extraction Results for the Fifth Dataset

The fifth dataset was also used to compare the different methods of mountain vertex extraction. The distribution graphs of Mountain Vertices extracted using each method are shown in the subsequent figures. Figure 25 shows the accurate mountain vertex distribution map extracted using the reference method. Figure 26a shows the distribution map using the Contour Line Extraction procedure, Figure 26b using the Neighborhood Analysis Method, and Figure 26c using the Contour Line and Neighborhood Analysis Overlay Method. The

distribution map of mountain vertices extracted using our proposed approach is provided in Figure 27.

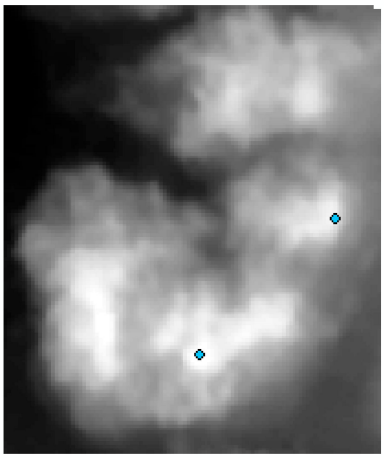

Figure 25. The distribution map of the fifth dataset extracted using the reference method.

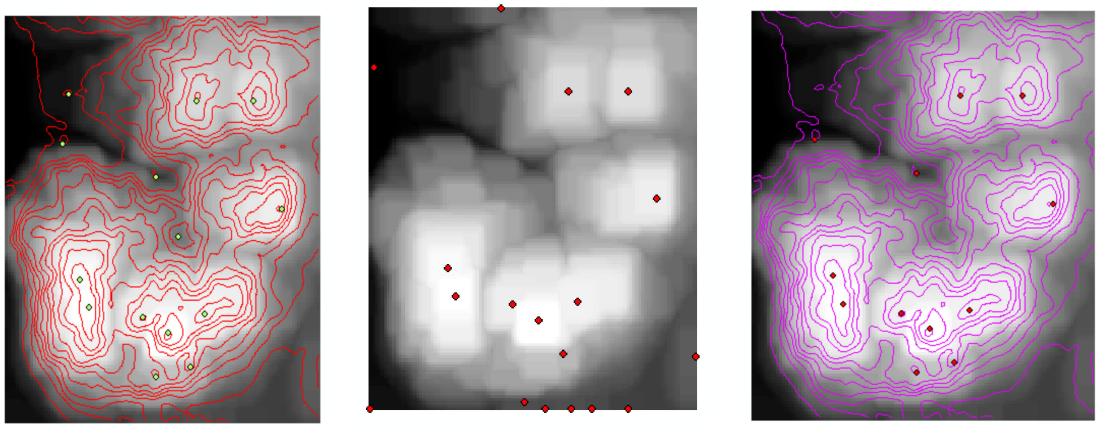

(**a**) (**b**) (**c**)

Figure 26. Distribution maps extracted by the traditional Mountain Vertices Extraction Methods using the fifth dataset. (**a**) Contour Line Method. (**b**) Neighborhood Analysis Method. (**c**) Contour line and Neighborhood Analysis Overlay Method.

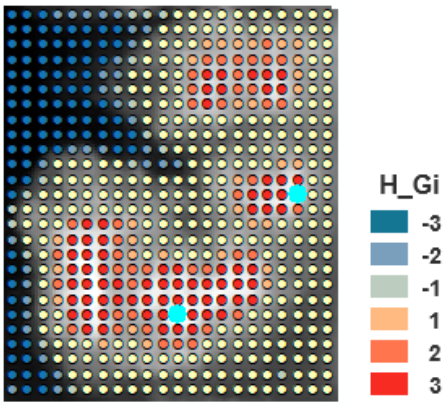

Figure 27. The distribution map for the fifth dataset using our proposed approach.

The extraction results using the different mountain vertex extraction methods were evaluated using the resulting extraction accuracy rates. The summary of results is provided in Table 16.

Table 16. The mountain vertices extraction results for each method using the fifth dataset.

Method	Extract NUM	Correct NUM	False NUM	Extract Rate	Correct Rate
Reference Method	2	2	0	100%	100%
The Proposed Method	2	2	0	100%	100%
CLM	15	2	1	13%	50%
NAM	18	2	0	11%	100%
CLaNAOM	12	2	0	16%	100%

As shown in Table 16, the Reference Method, the Proposed Method, the Contour Line Method, the Neighborhood Analysis Method, and the Contour Line and Neighborhood Analysis Overlay Method were used to process the fifth dataset. The number of extracted mountain vertices are 2, 2, 15, 18, and 12, and the accuracy rates are 100%, 100%, 50%, 100%, and 100%. The comparative analysis shows that the Reference Method and the Proposed Method yielded significantly better results.

3.6.3. Comparison of the Mountain Vertex Extraction Time Using Experimental Fifth Dataset

The time expended in extracting mountain vertices for the fifth dataset using our proposed approach and using the Contour Line and Neighborhood Analysis Overlay Method were recorded and compared. Table 17 shows the time consumed in extracting mountain vertices for the fifth dataset using our proposed approach, while Table 18 shows time results using the Contour Line and Neighborhood Analysis Overlay Method.

Table 17. The time consumed in extracting mountain vertices for the fifth dataset using our proposed approach.

NO.	Method	Time
1	Resampling of the Raster DEM by 10 × 10 pixel-size	0.08 s
2	Raster DEM conversion into point vector DEM	0.09 s
3	Hotspot analysis of the Point Vector DEM	0.12 s
4	Extraction of the mountain vertices	0.16 s
	Total Time	**0.45 s**

Table 18. The time spent in extracting mountain vertices for the fifth dataset using the Contour Line and Neighborhood Analysis Overlay Method.

NO.	Method	Time
1	Set 6 × 6 analysis window to neighborhood analyze the Raster DEM data	0.21 s
2	Generate 3 m interval contour lines for DEM data, extract the innermost contour line area	0.19 s
3	Calculate the intersection between the innermost circle of DEM and the neighborhood analysis obtain data to get the experimental fifth dataset's Mountain Vertices	0.12 s
	Total Time	**0.52 s**

The proposed method (the 10 × 10 resampling size) and the Contour Line and the Neighborhood Analysis Overlay Method (the 6 × 6 analysis window, the 3-m contour interval) were used for mountain vertex extraction for Dataset 5. The results show that the Proposed Method was 1.15 times faster than the Contour Line and Neighborhood Analysis Overlay Method for Dataset 5.

3.7. The Sixth Dataset: The Western Section of the West Area of Ji'an, China

3.7.1. Experimental Data Description

The sixth dataset consists of a raster DEM of Ji'an City, Jiangxi Province, China (longitude: 114.11°E–114.12°E, latitude: 27.18°N~27.19°N). As shown in Figure 28, the image has a 2 m spatial resolution, uses the CGCS2000 coordinate system, and has 146 rows and 136 columns. The terrain is characterized by low mountains, with an average altitude of 59–106 m and a height difference of about 47 m. Figure 28 shows the data and results for Dataset 6: (a) is the Digital Orthophoto Map (DOM), (b) is the Digital Elevation Model (DEM), and (c) is the hillshading results.

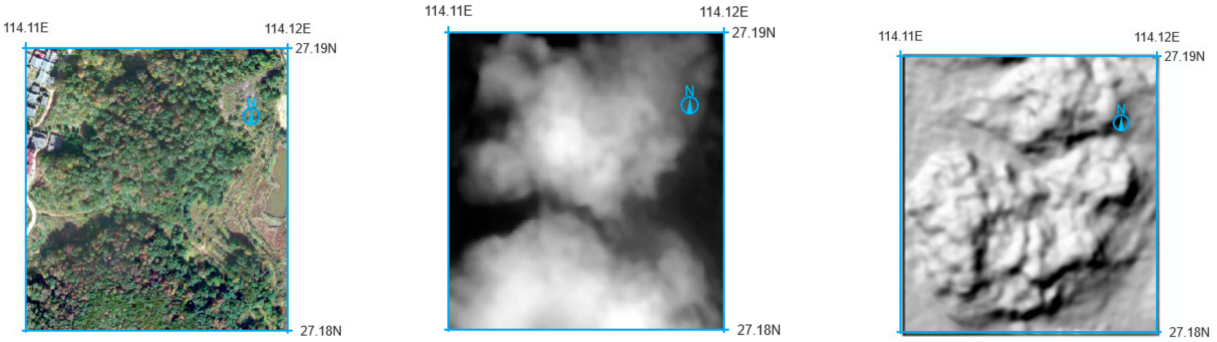

(**a**) DOM data of the sixth ataset (the western part of Ji'an, China)

(**b**) DEM data of the sixth dataset (the western part of Ji'an, China)

(**c**) Hillshading result of the sixth dataset (the western part of Ji'an, China)

Figure 28. The experimental sixth dataset:(**a**) DOM data of the sixth dataset (western part of Ji'an, China); (**b**) DEM data of the sixth dataset (western part of Ji'an, China); (**c**) Hillshading result of the sixth dataset (western part of Ji'an, China).

3.7.2. Comparison of the Mountain Vertex Extraction Results for the Sixth Dataset

The sixth dataset was also used to compare the different methods of mountain vertex extraction. The distribution graphs of Mountain Vertices extracted by each method are shown in the following figures. Figure 29 shows the accurate mountain vertex distribution map extracted using the reference method. Figure 30a shows the distribution map using the Contour Line Extraction procedure, Figure 30b using the Neighborhood Analysis Method, and Figure 30c using the Contour Line and Neighborhood Analysis Overlay Method. The distribution map of mountain vertices extracted using our proposed approach is provided in Figure 31.

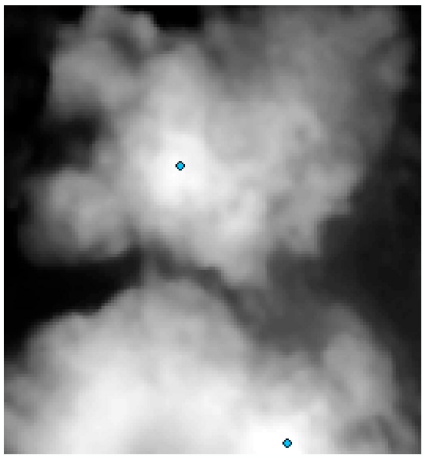

Figure 29. The distribution map of the sixth dataset extracted using the reference method.

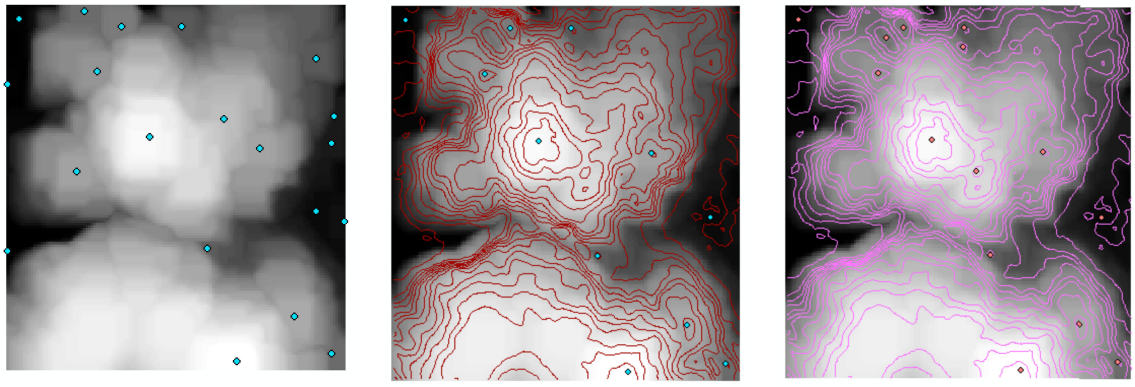

(**a**) (**b**) (**c**)

Figure 30. Distribution maps extracted by the traditional Mountain Vertices Extraction Methods using the sixth dataset. (**a**) Contour Line Method. (**b**) Neighborhood Analysis Method. (**c**) Contour line and Neighborhood Analysis Overlay Method.

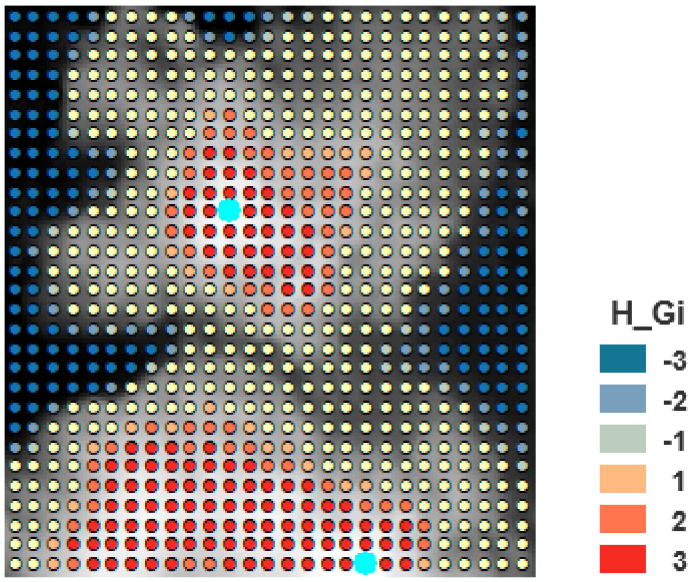

Figure 31. The distribution map for the sixth dataset using our proposed approach.

The extraction results using the different mountain vertex extraction methods were evaluated in terms of the extraction rate the resulting accuracy. The summary of results is provided in Table 19.

Table 19. The mountain vertices extraction results for each method using the sixth dataset.

Method	Extract NUM	Correct NUM	False NUM	Extract Rate	Correct Rate
The Reference Method	2	2	0	100%	100%
The Proposed Method	2	2	0	100%	100%
CLM	14	2	0	14%	100%
NAM	19	2	0	11%	100%
CLaNAOM	11	2	0	18%	100%

Table 19 shows the sixth district's vertex extraction results using the Reference Method, the Proposed Method, the Contour Line Method, the Neighborhood Analysis Method, and the Contour Line and Neighborhood Analysis Overlay Method. The number the mountain vertices extracted are 2, 2, 14, 19, and 11, and the accuracy rates are 100%, 100%, 14%, 11%, and 18%. The Reference Method and the Proposed Method yielded considerably better results.

3.7.3. Comparison of the Mountain Vertex Extraction Time Using Experimental the Sixth Dataset

The time expended in extracting mountain vertices for the sixth dataset using our proposed approach and using the Contour Line and Neighborhood Analysis Overlay Method were recorded and compared. Table 20 shows the time consumed in extracting mountain vertices for the sixth dataset using our proposed approach, while Table 21 shows time results using the Contour Line and Neighborhood Analysis Overlay Method.

Table 20. The time consumed in extracting mountain vertices for the sixth dataset using our proposed approach.

NO.	Method	Time
1	Resampling of the Raster DEM by 10 × 10 pixel-size	0.11 s
2	Raster DEM conversion into point vector DEM	0.13 s
3	Hotspot analysis of the Point Vector DEM	0.17 s
4	Extraction of the mountain vertices	0.22 s
	Total Time	**0.63 s**

Table 21. The time spent in extracting mountain vertices for the sixth dataset using the Contour Line and Neighborhood Analysis Overlay Method.

NO.	Method	Time
1	Set 6 × 6 analysis window to neighborhood analyze the Raster DEM data	0.29 s
2	Generate 3 m interval contour lines for DEM data, extract the innermost contour line area	0.27 s
3	Calculate the intersection between the innermost circle of DEM and the neighborhood analysis obtain data to get the experimental sixth dataset's mountain vertices	0.17 s
	Total Time	**0.73 s**

The proposed method (the 10 × 10 resampling size) and the Contour Line and the Neighborhood Analysis Overlay Method (the 6 × 6 analysis window, the 3 m contour interval) were used to extract the mountain vertices for Dataset 6. The results show that the

Proposed Method was 1.15 times faster than the Contour Line and Neighborhood Analysis Overlay Method for Dataset 6.

3.8. The Seventh Dataset: The Western Section of Zhou'shan, China

3.8.1. Experimental Data Description

Dataset 7 consists of a raster DEM of Zhou'shan City, Zhejiang Province, China (longitude: 122.03°E–122.16°E, latitude: 30.06°N~30.16°N). In Figure 32, the image has a 2 m spatial resolution, uses the CGCS2000 coordinate system, and has 6000 rows and 6000 columns. The terrain is characterized by high mountains, with an average altitude of −888~522 m and a height difference of about 1410 m. Figure 32 shows the data and results for Dataset 7: (a) is the Digital Orthophoto Map (DOM), (b) is the Digital Elevation Model (DEM), and (c) is the hillshading results.

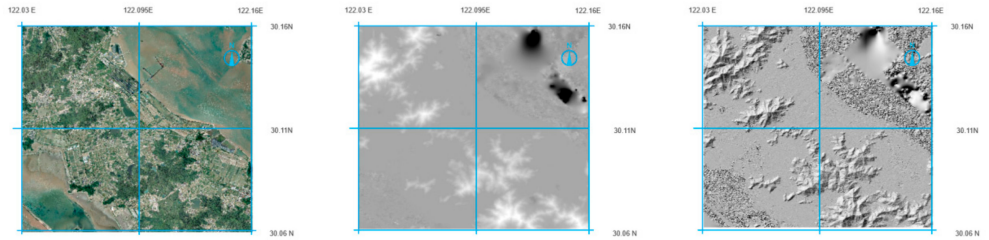

(**a**) DOM data of the seventh dataset (the western part of Zhou'shan, China)

(**b**) DEM data of the seventh dataset (the western part of Zhou'shan, China)

(**c**) Hillshading result of the seventh dataset (the western part of Zhou'shan, China)

Figure 32. The experimental seventh dataset:(**a**) DOM data of the seventh dataset (western part of Zhou'shan, China); (**b**) DEM data of the seventh dataset (western part of Zhou'shan, China); (**c**) Hillshading result of the seventh dataset (western part of Zhou'shan, China).

3.8.2. Comparison of the Mountain Vertex Extraction Results for the Seventh Dataset

Dataset 7 was also used to compare the different methods of mountain vertex extraction. The distribution graphs for each mountain extraction method are shown in the following figures. Figure 33 shows the distribution map extracted using the reference method. Figure 34a shows the distribution map using the Contour Line Extraction procedure, Figure 34b using the Neighborhood Analysis Method, and Figure 34c using the Contour Line and Neighborhood Analysis Overlay Method. The distribution map of mountain vertices extracted using our proposed approach is provided in Figure 35.

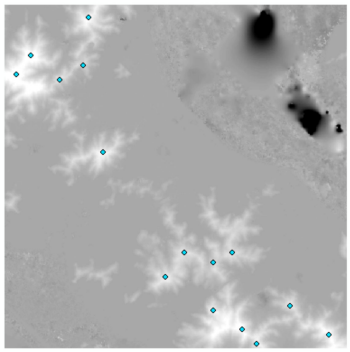

Figure 33. The distribution map of the seventh dataset extracted using the reference method.

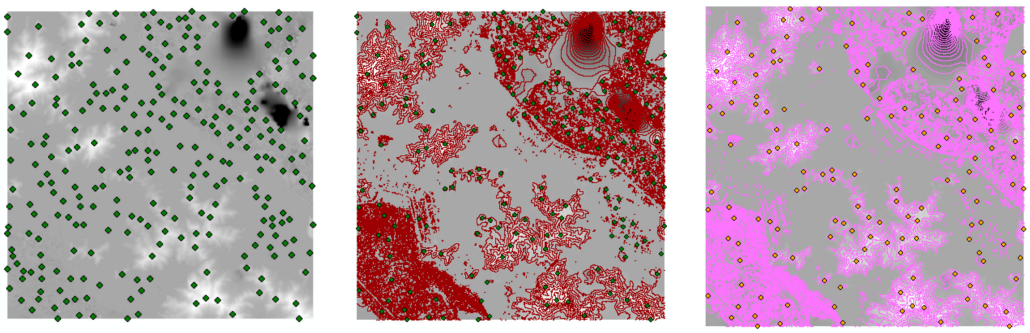

(**a**) (**b**) (**c**)

Figure 34. Distribution maps extracted by the traditional Mountain Vertices Extraction Methods using the seventh dataset. (**a**) Contour Line Method. (**b**) Neighborhood Analysis Method. (**c**) Contour line and Neighborhood Analysis Overlay Method.

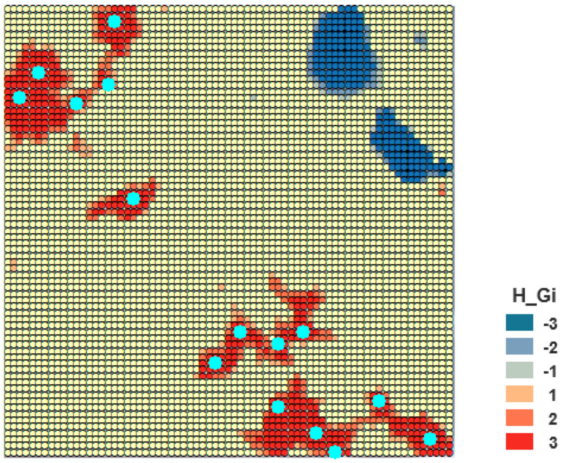

Figure 35. The distribution map for the seventh dataset using our proposed approach.

The extraction results using the different mountain vertex extraction methods were evaluated in terms of the extraction rate the resulting accuracy. The summary of results is provided in Table 22.

Table 22. The mountain vertices extraction results for each method using the seventh dataset.

Method	Extract NUM	Correct NUM	False NUM	Extract Rate	Correct Rate
The Reference Method	15	15	0	100%	100%
The Proposed Method	15	15	0	100%	100%
CLM	180	12	3	7%	80%
NAM	240	13	2	5%	87%
CLaNAOM	120	13	2	11%	87%

Table 22 shows Dataset 7's vertex extraction results using the Reference Method, the Proposed Method, the Contour Line Method, the Neighborhood Analysis Method, and the Contour Line and Neighborhood Analysis Overlay Method. The number the mountain vertices extracted are 15, 15, 12, 13, and 13, and the accuracy rates are 100%, 100%, 7%, 5%, and 11%. The Reference Method and the Proposed Method yielded considerably better results.

3.8.3. Comparison of the Mountain Vertex Extraction Time Using Experimental the Seventh Dataset

The time expended in extracting mountain vertices for Dataset 7 using our proposed approach and the Contour Line and Neighborhood Analysis Overlay Method were recorded and compared. Table 23 shows the time consumed in extracting mountain vertices for Dataset 7 using our proposed approach, while Table 24 shows time results for the Contour Line and Neighborhood Analysis Overlay Method.

Table 23. The time consumed in extracting mountain vertices for the seventh dataset using our proposed approach.

NO.	Method	Time
1	Resampling of the Raster DEM by 10 × 10 pixel-size	14.4 s
2	Raster DEM conversion into point vector DEM	14 s
3	Hotspot analysis of the Point Vector DEM	28.6 s
4	Extraction of the mountain vertices	38.6 s
	Total Time	**95.6 s**

Table 24. The time spent in extracting mountain vertices for the seventh dataset using the Contour Line and Neighborhood Analysis Overlay Method.

NO.	Method	Time
1	Set 6 × 6 analysis window to neighborhood analyze the Raster DEM data	58.2 s
2	Generate 3 m interval contour lines for DEM data, extract the innermost contour line area	53.4 s
3	Calculate the intersection between the innermost circle of DEM and the neighborhood analysis obtain data to get the experimental seventh dataset's mountain vertices	34.1 s
	Total Time	**145.7 s**

The proposed method (the 10 × 10 resampling size) and the Contour Line and the Neighborhood Analysis Overlay Method (the 6 × 6 analysis window, the 3 m contour interval) were used to extract the mountain vertices for Dataset 7. The experimental results show that the Proposed Method was 1.5 times faster than the Contour Line and Neighborhood Analysis Overlay Method for Dataset 7.

3.9. Discussion

The method proposed in this paper combines the Hotspot Analysis Clustering Algorithm and the Improved Eight-Connected Extraction Algorithm in order to determine the location and elevation of mountain vertices fast and accurately. After conducting a comparative assessment of the proposed approach against traditional extraction procedures, the results show our approach yielded higher extraction efficiency compared to the Contour Line Method, Neighborhood Analysis Method, and the Contour Line and Neighborhood Analysis Overlay Method.

In the first experiment (Dataset 1), our proposed method's extraction rate was 55% higher than the Contour Line and Neighborhood Analysis Overlay Method, 86% higher than the Contour Line Method, and 87.5% higher than the Neighborhood Analysis Method. In the second experiment (Dataset 2), the extraction rate of our proposed approach was 67% higher than the Contour Line and Neighborhood Analysis Overlay method, 81% higher than the Contour Line Method, and 85% higher than the Neighborhood Analysis Method. In the third experiment (Dataset 3), our proposed method's extraction rate was 92.7% higher than the Contour Line and Neighborhood Analysis Overlay Method, 93.7% higher than the Contour Line Method, and 88.2% higher than the Neighborhood Analysis

Method. In the fourth experiment (Dataset 4), our proposed method's extraction rate was 94% higher than the Contour Line and Neighborhood Analysis Overlay Method, 95.7% higher than the Contour Line Method, and 92.6% higher than the Neighborhood Analysis Method. In the fifth experiment (Dataset 5), our proposed method's extraction rate was 84% higher than the Contour Line and Neighborhood Analysis Overlay Method, 87% higher than the Contour Line Method, and 89% higher than the Neighborhood Analysis Method. In the sixth experiment (Dataset 6), our proposed method's extraction rate was 86% higher than the Contour Line and Neighborhood Analysis Overlay Method, 89% higher than the Contour Line Method, and 82% higher than the Neighborhood Analysis Method. In the seventh experiment (Dataset 7), our proposed method's extraction rate was 89% higher than the Contour Line and Neighborhood Analysis Overlay Method, 93% higher than the Contour Line Method, and 95% higher than the Neighborhood Analysis Method, as shown in Table 25.

Table 25. The extraction rate in each method for Datasets 1–7.

Method	Dataset-1	Dataset-2	Dataset-3	Dataset-4	Dataset-5	Dataset-6	Dataset-7
The Proposed Method	100%	100%	100%	100%	100%	100%	100%
CLM	14%	19%	7.3%	6%	13%	14%	7%
NAM	12.5%	15%	6.3%	4.3%	11%	11%	5%
CLaNAOM	45%	33%	11.8%	7.4%	16%	18%	11%

The accuracy rate of our proposed extraction method was also comparatively higher than the other methods. For Dataset 1, the accuracy rate of the proposed approach was 20% higher than the Contour Line and Neighborhood Analysis Overlay Method, 20% higher than the Neighborhood Analysis Method, and 40% higher than the Contour Line Method. Using Dataset 2, the accuracy rate of the proposed method was 20% higher than the Contour Line and Neighborhood Analysis Overlay Method, 20% higher than the Neighborhood Analysis Method, and 40% higher than the Contour Line Method. For Dataset 3, the accuracy rate of the proposed approach was 20% higher than the Contour Line and Neighborhood Analysis Overlay Method, 20% higher than the Neighborhood Analysis Method, and 40% higher than the Contour Line Method. For Dataset 4, the accuracy rate of the proposed approach was 20% higher than the Contour Line and Neighborhood Analysis Overlay Method, 20% higher than the Neighborhood Analysis Method, and 20% higher than the Contour Line Method. For Dataset 5, the accuracy rate of the proposed approach was 50% higher than the Contour Line Method. For Dataset 7, the accuracy rate of the proposed approach was 13% higher than the Contour Line and Neighborhood Analysis Overlay Method, 13% higher than the Neighborhood Analysis Method, and 20% higher than the Contour Line Method. These results suggest that the proposed method is able to provide high accuracy extraction results and is able to effectively eliminate the interference of invalid points. When compared to traditional vertex-extraction techniques, the proposed approach was able to maintain high accuracy and was comparatively more efficient, requiring less processing and computing time than the other methods, as shown in Table 26.

Table 26. The accuracy rate for each method using in the first to seventh dataset to extract the mountain vertices.

Method	Dataset-1	Dataset-2	Dataset-3	Dataset-4	Dataset-5	Dataset-6	Dataset-7
The Proposed Method	100%	100%	100%	100%	100%	100%	100%
CLM	60%	60%	60%	80%	50%	100%	80%
NAM	80%	80%	80%	80%	100%	100%	87%
CLaNAOM	80%	80%	80%	80%	100%	100%	87%

4. Conclusions

DEM-based extraction of the mountain vertices is an important and useful technique in characterizing topographic features and has become one of the most useful DEM applications. Current vertex-extraction techniques have considerable challenges and limitations. For instance, the Contour Line Method often yield low-accuracy extraction results, while the Neighborhood Analysis Method produces significant false or erroneous mountain vertices. To overcome these limitations, this study proposes a new approach that combines Hotspot Analysis Clustering and the Improved Eight-Connected Extraction algorithms in order to quickly and accurately obtain the location and elevation of mountain vertices. The main processing procedures are as follows: First, the raster DEM must be preprocessed. Then, using Getis-Ord Gi* Method, hotspot analysis and clustering are performed to define the hotspot and the cold-spot based on the differences between the calculated *p*-value and Z-score. The DEM hotspot image can then be generated, and areas of high and low-values can be properly demarcated. Finally, the Improved Eight-Connected Extraction Algorithm is used to extract the accurate position and elevation of mountain vertices from the DEM hotspot image.

Compared with traditional mountain vertex extraction methods, the proposed approach was shown to achieve positive results. Our experimental results show that the proposed approach maintained high extraction accuracy, significantly minimized the occurrence of invalid points, and obtained the precise location and elevation of mountain vertices more efficiently.

Author Contributions: Z.Z., X.X., Z.-C.Z., Y.Z., J.T. and D.L. proposed the idea and wrote the manuscript; Z.Z., X.X., Z.-C.Z., Y.Z., N.Y. and J.T. designed and performed experiments; X.X. and Y.Z. helped to revise the manuscript. All authors have read and agreed to the published version of the manuscript.

Funding: This research was funded by the National Natural Science Foundation of China (Grant Nos. 91638203, 91738302), Fundamental Research Funds for the Central Universities of China (Grant No. 2042019kf0002), the Land Resources Research Project of Hubei Province (No. 2018-844-11), China Scholarship Council (Grant No. 201606270125), the Science and Technology Program of Southwest China Research Institute of Electronic Equipment (Grant No. JS20200500114), the Science and Technology Program of Guangzhou, China (Grant No. 2017010160173) and LIESMARS Special Research Funding.

Acknowledgments: Thanks to Kun Xie at the Wuhan Xuntu Technology Co. Ltd. for providing us the several sets of experimental data. We are thankful to Stephen C. McClure for providing us English editing of the manuscript freely.

Conflicts of Interest: The authors declare no conflict of interest.

Nomenclature

In this section, we explain all the abbreviations of this paper. The Nomenclature explanation is specified in follow

DEM	Digital Elevation Model
DOM	Digital Orthophoto Map
CLM	Contour Line Method
NAM	Neighborhood Analysis Method
CLaNAOM	Contour Line and Neighborhood Analysis Overlay Method
NUM	Number

References

1. Mukherjee, S.; Joshi, P.K.; Mukherjee, S.; Ghosh, A.; Garg, R.; Mukhopadhyay, A. Evaluation of vertical accuracy of open source Digital Elevation Model (DEM). *Int. J. Appl. Earth Obs. Geoinf.* **2013**, *21*, 205–217. [CrossRef]
2. Pathmanabhan, A.; Dinesh, S. The effect of Gaussian blurring on the extraction of peaks and pits from digital elevation models. *Discret. Dyn. Nat. Soc.* **2007**, *2007*, 149–174. [CrossRef]

3. Mansoori, S.A.; Al-Ruzouq, R.; Dogom, D.A.; Shamsi, M.A.; Mazzm, A.A.; Aburaed, N. Photogrammetric techniques and UAV for drainage pattern and overflow assessment in mountainous Terrains-Hatta/UAE. In Proceedings of the IGARSS 2019–2019 IEEE International Geoscience and Remote Sensing Symposium, Yokohama, Japan, 28 July–2 August 2019; pp. 951–954.
4. Remondino, F.; Barazzetti, L.; Nex, F.; Scaioni, M.; Sarazzi, D. UAV photogrammetry for mapping and 3d modeling–current status and future perspectives. In Proceedings of the International Conference on Unmanned Aerial Vehicle in Geomatics (UAV-g), Zurich, Switzerland, 14–16 September 2011; pp. 1–7.
5. Ghuffar, S. DEM generation from multi satellite planetscope imagery. *Remote Sens.* **2018**, *10*, 1462. [CrossRef]
6. Wang, T.; Somani, A.K. Aerial-DEM geolocalization for GPS-denied UAS navigation. *Mach. Vis. Appl.* **2020**, *31*, 3.1–3.12. [CrossRef]
7. Akturk, E.; Altunel, A.O. Accuracy assessment of a low-cost UAV derived digital elevation model (DEM) in a highly broken and vegetated terrain. *Measurement* **2019**, *136*, 382–386. [CrossRef]
8. Abdallah, A.; Saifeldin, A.; Abomariam, A.; Ali, R. Efficiency of using GNSS-PPP for digital elevation model (DEM) production. *Artif. Satell.* **2020**, *55*, 17–28. [CrossRef]
9. Middleton, M.; Heikkonen, J.; Nevalainen, P.; Hyvönen, E.; Sutinen, R.J.G. Machine learning-based mapping of micro-topographic earthquake-induced paleo-Pulju moraines and liquefaction spreads from a digital elevation model acquired through laser scanning. *Geomorphology* **2020**, *358*. [CrossRef]
10. Tian, W.; Zhao, Z.; Hu, C.; Wang, J.; Zeng, T. GB-InSAR-Based DEM generation method and precision analysis. *Remote Sens.* **2019**, *11*, 997. [CrossRef]
11. Zhao, M. An indirect interpolation model and its application for digital elevation model generation. *Earth Sci. Inf.* **2020**, *13*, 1251–1264. [CrossRef]
12. Lun, W.; Yu, L. *Geographic Information Systems: Principles, Methods and Applications*, 2nd ed.; Publisher Peking: Beijing, China, 2001; pp. 195–214.
13. Xiuwen, W. Research on Geomorphology Analysis Base on DEM. Master's Thesis, Nanjing Normal University, Nanjing, China, 2006.
14. Mokarram, M.; Hojati, M. Morphometric analysis of stream as one of resources for agricultural lands irrigation using high spatial resolution of digital elevation model (DEM). *Comput. Electron. Agric.* **2017**, *142*, 190–200. [CrossRef]
15. Li, S.; Huanwei, C.; Jiawen, P. Analysis of the land use spationtemporal variation base on DEM. *J. Mt. Sci.* **2004**, *6*, 762–766.
16. Zheng, X.; Xiong, H.; Gong, J.; Yue, L. A robust channel network extraction method combining discrete curve evolution and the skeleton construction technique. *Adv. Water Resour.* **2015**, *83*, 17–27. [CrossRef]
17. Bolch, T.; Pieczonka, T.; Mukherjee, K.; Shea, J.M. Brief communication: Glaciers in the Hunza catchment (Karakoram) have been nearly in balance since the 1970s. *Cryosphere* **2017**, *11*, 531–539. [CrossRef]
18. Næsset, E.; Ørka, H.O.; Solberg, S.; Bollandsås, O.M.; Hansen, E.H.; Mauya, E.; Zahabu, E.; Malimbwi, R.; Chamuya, N.; Olsson, H. Mapping and estimating forest area and aboveground biomass in miombo woodlands in Tanzania using data from airborne laser scanning, TanDEM-X, RapidEye, and global forest maps: A comparison of estimated precision. *Remote Sens. Environ.* **2016**, *175*, 282–300. [CrossRef]
19. Zhang, Z.; Lu, X.; Zhou, M.; Song, Y.; Luo, X.; Kuang, B. Complex spatial morphology of urban housing price based on digital elevation model: A case study of Wuhan city, China. *Sustainability* **2019**, *11*, 348. [CrossRef]
20. Zonghua, L. Research on the Construction and Application of Spatial Data Infrastructure of Digital City. Ph.D. Thesis, Wuhan University, Wuhan, China, 1974.
21. Podobnikar, T. Detecting mountain peaks and delineating their shapes using digital elevation models, remote sensing and geographic information systems using autometric methodological procedures. *Remote Sens.* **2012**, *4*, 784–809. [CrossRef]
22. Zhu, H.; Zhao, Y.; Liu, H. Scale characters analysis for gully structure in the watersheds of loess landforms based on digital elevation models. *Front. Earth Sci.* **2018**, *12*, 431–443. [CrossRef]
23. Ma, S.; Qiu, H.; Hu, S.; Yang, D.; Liu, Z. Characteristics and geomorphology change detection analysis of the Jiangdingya landslide on July 12, 2018, China. *Landslides* **2020**, *17*, 1–14. [CrossRef]
24. Bolongaro-Crevenna, A.; Torres-Rodríguez, V.; Sorani, V.; Frame, D.; Ortiz, M.A. Geomorphometric analysis for characterizing landforms in Morelos State, Mexico. *Geomorphology* **2005**, *67*, 407–422. [CrossRef]
25. Peizhi, H.; Zehui, L. Study of extraction of ridge and valley from DEM data. *Bull. Surv. Mapp.* **2005**, *4*, 11–13.
26. Wenyuan, Y. The Analysis and Application of Terrain Features from DEM. Master's Thesis, Xi'an University of Architecture and Technology, Xi'an, China, 2010.
27. Shuqiong, L.; Shilin, Z.; Shengwu, Z.; Liangzhu, H. Extracting mountain peaks based on grid DEM. *J. East China Inst. Technol.* **2013**, *36*, 93–95.
28. Panpan, C. A Research on Surface Peaks and Its Attribution's Spatial Distributing Based on DEM in Shanxi Province. Master's Thesis, Northwest University, Xi'an, China, 2006.
29. Erskine, R.H.; Green, T.R.; Ramirez, J.A.; MacDonald, L.H. Digital elevation accuracy and grid cell size: Effects on estimated terrain attributes. *Soil Sci. Soc. Am. J.* **2007**, *71*, 1371–1380. [CrossRef]
30. Gu, L.; Wang, C.; Li, P.; Wang, J.; Wang, Z. Research on mountain top extraction accuracy based on DEM. *Geomat. Inf. Sci. Wuhan Univ.* **2016**, *41*, 131–135.
31. Wenjuan, W. Topographic Feature Line Extraction of Regular Grid DEM. Master's Thesis, Chang'an University, Xi'an, China, 2018.

32. Gioia, D.; Danese, M.; Bentivenga, M.; Pescatore, E.; Siervo, V.; Giano, S.I. Comparison of different methods of automated landform classification at the drainage basin scale: Examples from the Southern Italy. In Proceedings of the International Conference on Computational Science and Its Applications, Springer, Cham, 1–4 July 2020; pp. 696–708.
33. Li, Y.; Lei, N.; Xiong, Y. Research on watershed extraction method based on GIS. In Proceedings of the IOP Conference Series: Earth and Environmental Science, Prague, Czech Republic, 3–7 September 2018; p. 022168.
34. Ma, H.; Zhou, W.; Zhang, L. DEM refinement by low vegetation removal based on the combination of full waveform data and progressive TIN densification. *ISPRS J. Photogramm. Remote Sens.* **2018**, *146*, 260–271. [CrossRef]
35. Hongjian, L.; Jianzhong, L.; Zhongxiang, C.; Linxiang, Z. A method of peak extraction by DEM based on basin subdivision. *J. Geom. Sci. Technol.* **2014**, *31*, 119–122.
36. Liu, X.; Jin, B.; Wang, Y. Similarity analysis of flow route algorithms for extracting drainage network from grid-based terrain model. *Geogr. Res.* **2008**, *06*, 1347–1357.
37. Luo, M.; Tang, G. Mountain peaks extraction based on geomorphology cognitive and space segmentation. *Sci. Surv. Mapp.* **2010**, *35*, 126–127.
38. Yueping, K.; Yanjun, Q.; Jing, J.; Wen, N. Mountain peak extraction based on topological analysis of mountain control area. *J. Geom. Sci. Technol.* **2018**, *1*, 77–81.
39. Guifang, H.; Minshi, L.; Lifan, F. Peak extraction from contour based on the improved AKIMA Algorithm. *J. Geom. Sci. Technol.* **2019**, *36*, 400–405.
40. Yue, M.; Yingjin, S.; Wenshi, Z.; Xin, K.; Peng, Z. Method of peak extraction based on spatial subdivision. *J. Geom. Sci. Technol.* **2015**, *32*, 433–437.
41. Spatial-Statistics: How the Hot Spot Analysis (Getis-Ord Gi) Works. Available online: https://pro.arcgis.com/en/pro-app/tool-reference/spatial-statistics/h-how-hot-spot-analysis-getis-ord-gi-spatial-stati.htm (accessed on 1 June 2019).
42. Spatial-Statistics: What's a Z-Score, What's a p-Value. Available online: https://desktop.arcgis.com/zh-cn/arcmap/latest/tools/spatial-statistics-toolbox/what-is-a-z-score-what-is-a-p-value.htm (accessed on 1 June 2019).
43. Hou, Q.; Zhang, X.; Li, B.; Zhang, X.; Wang, W. Applications. Identification of low-carbon travel block based on GIS hotspot analysis using spatial distribution learning algorithm. *Arab. J. Geosci.* **2019**, *31*, 4703–4713.
44. Peeters, A.; Zude, M.; Käthner, J.; Ünlü, M.; Kanber, R.; Hetzroni, A.; Gebbers, R.; Ben-Gal, A. Getis–Ord's hot-and cold-spot statistics as a basis for multivariate spatial clustering of orchard tree data. *Comput. Electron. Agric.* **2015**, *111*, 140–150. [CrossRef]
45. Xiajiong, S.; Jingjing, W. Labeling algorithm of 8-adjacent connecting area for massive gray scale images. *Comput. Egn. Appl.* **2013**, *49*, 126–129.
46. Li, M.; Zhao, L.; Tan, D.; Tong, X. BLE fingerprint indoor localization algorithm based on eight-neighborhood template matching. *Sensors* **2019**, *19*, 4859. [CrossRef]
47. He, C.; Li, X.; Hu, Y.; Ye, Z.; Kang, H. Microscope images automatic focus algorithm based on eight-neighborhood operator and least square planar fitting. *Optik* **2020**, *206*. [CrossRef]
48. Panpan, C.; Youshun, Z.; Chun, W.; Shanshan, G. Method of extracting surface peaks based on DEM. *Mod. Surv. Mapp.* **2006**, *29*, 11–13.